AEDC-TR-73-44
AFATL-TR-73-50

cy 3

AERODYNAMIC CHARACTERISTICS OF TWO BODIES OF REVOLUTION WITH NOSES OF VARYING SPHERICAL BLUNTNESS AT MACH NUMBERS FROM 0.6 TO 1.5

E. G. Allee, Jr.

ARO, Inc.

April 1973

PROPULSION WIND TUNNEL FACILITY
ARNOLD ENGINEERING DEVELOPMENT CENTER
AIR FORCE SYSTEMS COMMAND
ARNOLD AIR FORCE STATION, TENNESSEE

NOTICES

When U. S. Government drawings specifications, or other data are used for any purpose other than a definitely related Government procurement operation, the Government thereby incurs no responsibility nor any obligation whatsoever, and the fact that the Government may have formulated, furnished, or in any way supplied the said drawings, specifications, or other data, is not to be regarded by implication or otherwise, or in any manner licensing the holder or any other person or corporation, or conveying any rights or permission to manufacture, use, or sell any patented invention that may in any way be related thereto.

Qualified users may obtain copies of this report from the Defense Documentation Center.

References to named commercial products in this report are not to be considered in any sense as an endorsement of the product by the United States Air Force or the Government.

AERODYNAMIC CHARACTERISTICS OF TWO BODIES OF REVOLUTION WITH NOSES OF VARYING SPHERICAL BLUNTNESS AT MACH NUMBERS FROM 0.6 TO 1.5

E. G. Allee, Jr.
ARO, Inc.

FOREWORD

The work reported herein was conducted at the Arnold Engineering Development Center (AEDC) under the sponsorship of the Air Force Armament Laboratory (DLGC), Armament Development and Test Center, Air Force Systems Command (AFSC), Eglin Air Force Base, Florida, under Program Element 62602F, Project 2547.

The test results presented were obtained by ARO, Inc. (a subsidiary of Sverdrup & Parcel and Associates, Inc.), contract operator of AEDC, AFSC, Arnold Air Force Station, Tennessee. The work was performed from November 29 through December 13, 1972, under ARO Project No. PA278. The manuscript was submitted for publication on January 19, 1973.

This technical report has been reviewed and is approved.

L. R. KISSLING
Lt Colonel, USAF
Chief Air Force Test Director, PWT
Directorate of Test

A. L. COAPMAN
Colonel, USAF
Director of Test

ABSTRACT

A wind tunnel investigation was conducted in the Aerodynamic Wind Tunnel (1T) to determine the static stability characteristics of two bodies of revolution fitted with 2-, 3-, and 4-cal tangent ogive noses of varying spherical bluntness. Testing was conducted at Mach numbers from 0.6 to 1.5 and angles of attack from -2 to 14 deg. The major effect of blunting the noses was evidenced in the axial-force coefficient. Lengthening the noses from 2 to 4 cal caused a forward movement of the center-of-pressure location and a corresponding decrease in axial-force coefficient at Mach numbers of 1.0 and higher. Changing from a 5- to a 9-cal midbody resulted in an increase in axial-force coefficient and an aft movement of the center-of-pressure location.

CONTENTS

APPENDIX
ILLUSTRATIONS

NOMENCLATURE

C_A Axial-force coefficient, measured axial force/$q_\infty S$

$C_{A,b}$ Base axial-force coefficient, $(p_\infty - p_b)/q_\infty S$

$C_{A,F}$ Forebody axial-force coefficient, $C_A - C_{A,b}$

C_m Pitching-moment coefficient, measured pitching moment/$q_\infty S\bar{c}$

C_N Normal-force coefficient, measured normal force/$q_\infty S$

$\bar{c}$ Model moment reference length, 0.1 ft

M_∞ Free-stream Mach number

p_b Base pressure, psfa

p_∞ Free-stream static pressure, psfa

q_∞ Free-stream dynamic pressure, 0.7 $p_\infty M_\infty^2$, psf

S Model reference area, $\pi\bar{c}^2/4$, 0.07854 ft^2 .007854 Ft²

X_{CP} Center-of-pressure location, C_m/C_N, cal

X_{NP} Neutral-point location, $(dC_m/dC_N)_{\alpha=0}$, cal

α Model angle of attack, deg

Note: C_m, X_{CP}, and X_{NP} are all referenced to the model nose-body junction.

SECTION I
INTRODUCTION

A wind tunnel investigation was conducted in the Aerodynamic Wind Tunnel (1T), Propulsion Wind Tunnel Facility (PWT), to determine the static stability characteristics of two bodies of revolution when fitted with 2-, 3-, and 4-cal noses of varying spherical bluntness (defined as the ratio of spherical nose radius to body radius). The tests were conducted at Mach numbers from 0.6 to 1.5 and angles of attack from -2 to 14 deg.

The purpose of the test was to provide aerodynamic data for the preliminary design of guided munitions which require a spherical optical window in the nose.

SECTION II
APPARATUS

2.1 TEST FACILITY

The Aerodynamic Wind Tunnel (1T) is a continuous flow, non-return wind tunnel capable of being operated at Mach numbers from 0.2 to 1.5 utilizing variable nozzle contours above M_∞ = 1.1. The tunnel is operated at a stilling chamber total pressure of approximately 2850 psfa with ±5-percent variation, dependent on tunnel resistance and ambient atmospheric conditions. The total temperature can be varied from 80 to 120 deg above ambient as necessary to prevent visible condensation in the test section. The test section is 1 ft square and 37.5 in. long with six-percent open area perforated walls. A schematic of the tunnel installation is shown in Fig. 1 (Appendix). Photographs of a typical installation of both 5- and 9-cal midbodies are shown in Fig. 2.

2.2 TEST ARTICLES

The test models were composed of a tangent ogive nose (N), a cylindrical midbody (M), and a finless cylindrical afterbody (A) joined together to form a composite unit. Photographs of these components are presented in Fig. 3.

In this report, all configurations will be identified by this N-M-A nomenclature, e.g., N14 M5 A17. The various noses, midbodies, and afterbody, and their corresponding identification numbers, are specified in the dimensional sketches presented in Fig. 4. Twelve noses were tested on two centerbodies. The afterbody on all configurations was a 1-cal cylinder.

There were three basic tangent ogive nose lengths: 2, 3, and 4 cal. Each basic nose was modified by "rounding off" the tip to three different ratios of nose radius to body radius. The ratios used were 0.25, 0.50, and 0.75.

2.3 INSTRUMENTATION

A 6-component internal strain-gage balance was used to acquire aerodynamic forces and moments. In addition, base pressure was obtained by averaging the readings from two pressure transducers connected to orifices placed on either side of the sting (Fig. 2) at the plane of the model base.

SECTION III
TEST PROCEDURES

3.1 TEST CONDITIONS AND DATA ACQUISITION

Data were obtained on all configurations at Mach numbers of 0.6, 0.8, 1.0, 1.2, and 1.5 at angles of attack from -2 to 14 deg. Tunnel total temperature was varied from 150 to 200°F as required to prevent moisture condensation in the test section. Tunnel total pressure varied from 2780 to 2970 psfa. The resultant dynamic pressure varied from a minimum of 550 psf at M_∞ = 0.6 to a maximum of 1275 psf at M_∞ = 1.5.

3.2 PRECISION OF MEASUREMENTS

The accuracy of the data presented was affected by uncertainties in tunnel conditions and balance measurements. Uncertainties in the tunnel conditions and coefficient data were calculated for each data point as a part of the data reduction program. By assuming negligible bias and a 95-percent confidence level, typical results were as follow:

	Uncertainty					
M_∞	ΔM_∞	ΔQ (psf)	ΔC_N	ΔC_A	ΔC_m	ΔX_{CP}
0.6	0.004	6	0.03	0.03	0.03	0.06
0.8	0.005	6	0.02	0.02	0.02	0.04
1.0	0.006	5	0.02	0.02	0.02	0.03
1.2	0.008	4	0.01	0.01	0.01	0.02
1.5	0.010	2	0.01	0.01	0.01	0.02

SECTION IV
RESULTS

Data are presented for each nose-midsection-afterbody combination in Figs. 5 through 10. In general, rounding the nose to the 0.25, 0.50, and 0.75 ratios of spherical bluntness had negligible effect on the normal-force coefficient. The center-of-pressure location moved

aft on the model as the nose was blunted. The amount of movement varied with Mach number and basic nose length (2, 3, or 4 cal). As expected, the higher degrees of bluntness caused an increase in the forebody axial-force coefficients. This increase was most evident at M_∞ = 1.2 and 1.5.

Comparisons of 2-, 3-, and 4-cal noses of the same bluntness show changes in center-of-pressure location and forebody axial-force coefficient (Figs. 11 and 12). As the basic nose was lengthened, the center-of-pressure location moved forward. The effect of the longer noses on forebody axial-force coefficient was small at Mach numbers of 0.6 and 0.8. At Mach numbers of 1.0, 1.2, and 1.5, there was a decrease in the axial-force coefficient as the basic nose length was changed from 2 to 4 cal. The magnitude of this decrease became smaller as each basic nose was blunted from 0 to 0.75. At a bluntness ratio of 0.75, the difference in forebody axial-force coefficient among the three noses was small at all Mach numbers at which data were acquired.

A comparison of data for the same nose on the 5-cal (M5) and 9-cal (M9) midbodies shows an increase in forebody axial-force coefficient, a decrease in base axial-force coefficient, and an aft movement of the center-of-pressure location with the 9-cal midbody. Data taken with the 9-cal midbody showed a slightly higher normal-force coefficient than with the 5-cal midbody at angles of attack greater than 6 deg. Typical plots of these comparisons for noses of zero and 0.50 bluntness ratios are presented in Figs. 13 and 14.

APPENDIX
ILLUSTRATIONS

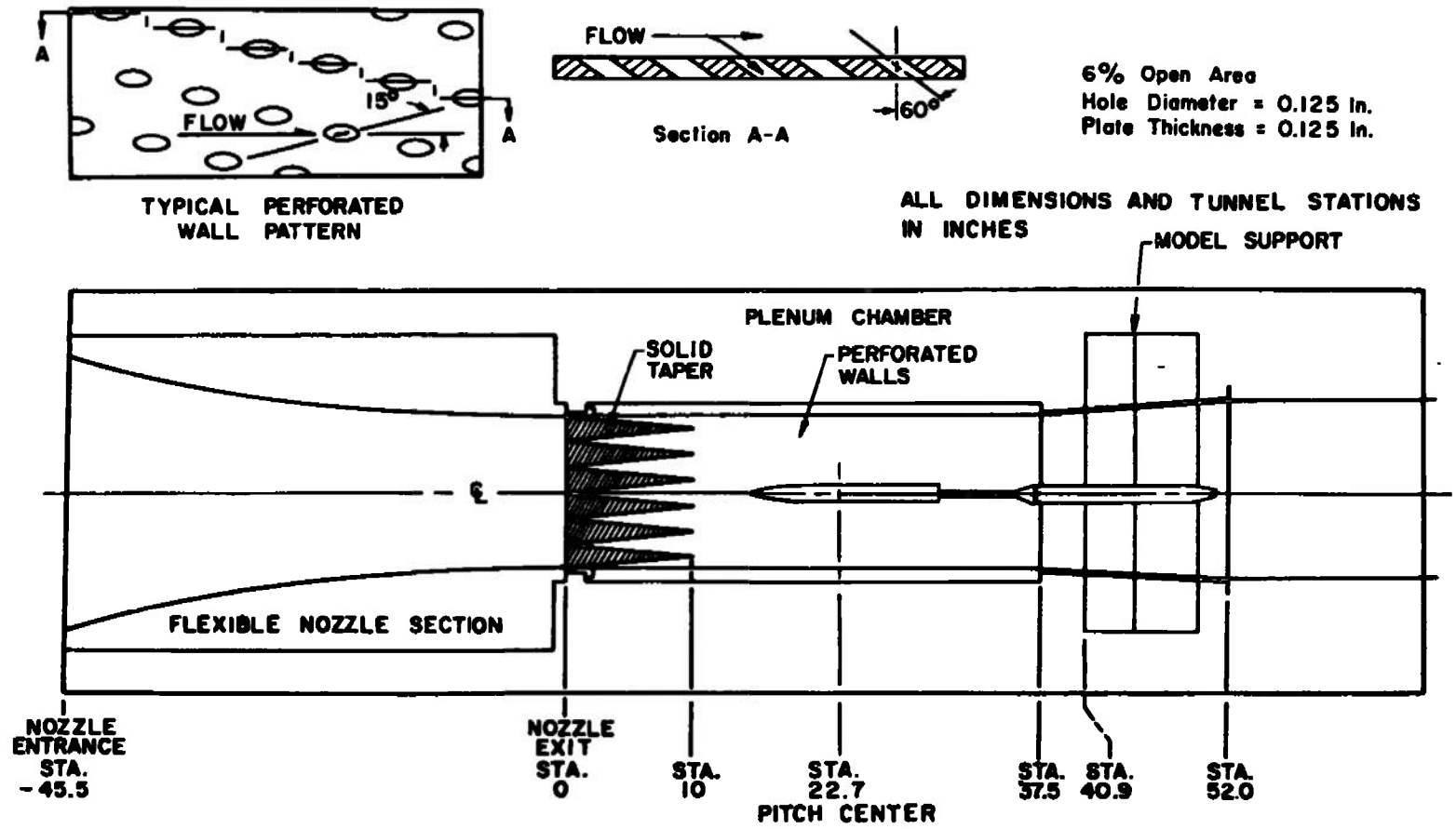

Fig. 1 Schematic of Test Installation

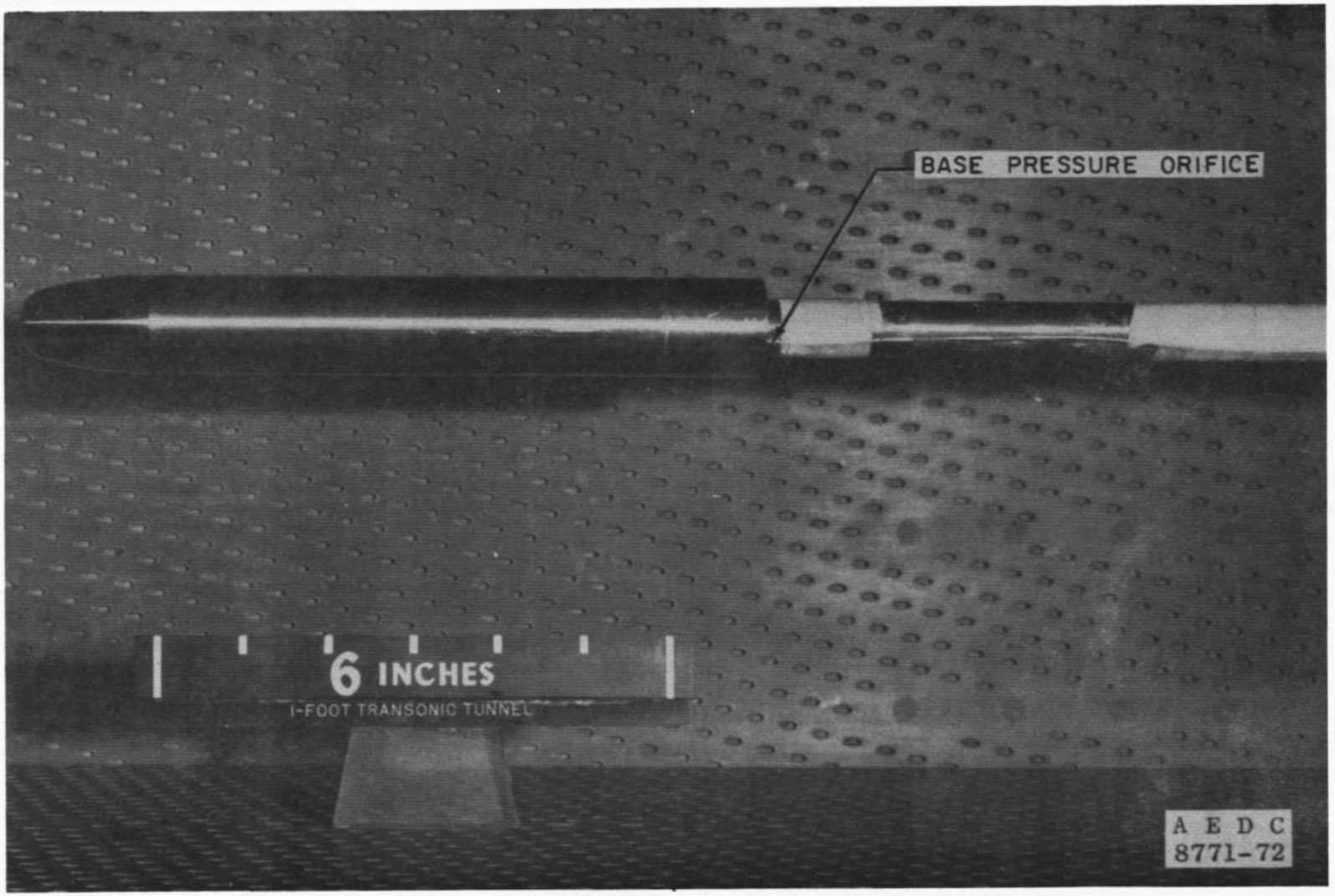

a. N17 M5 A17

Fig. 2 Installation Photographs

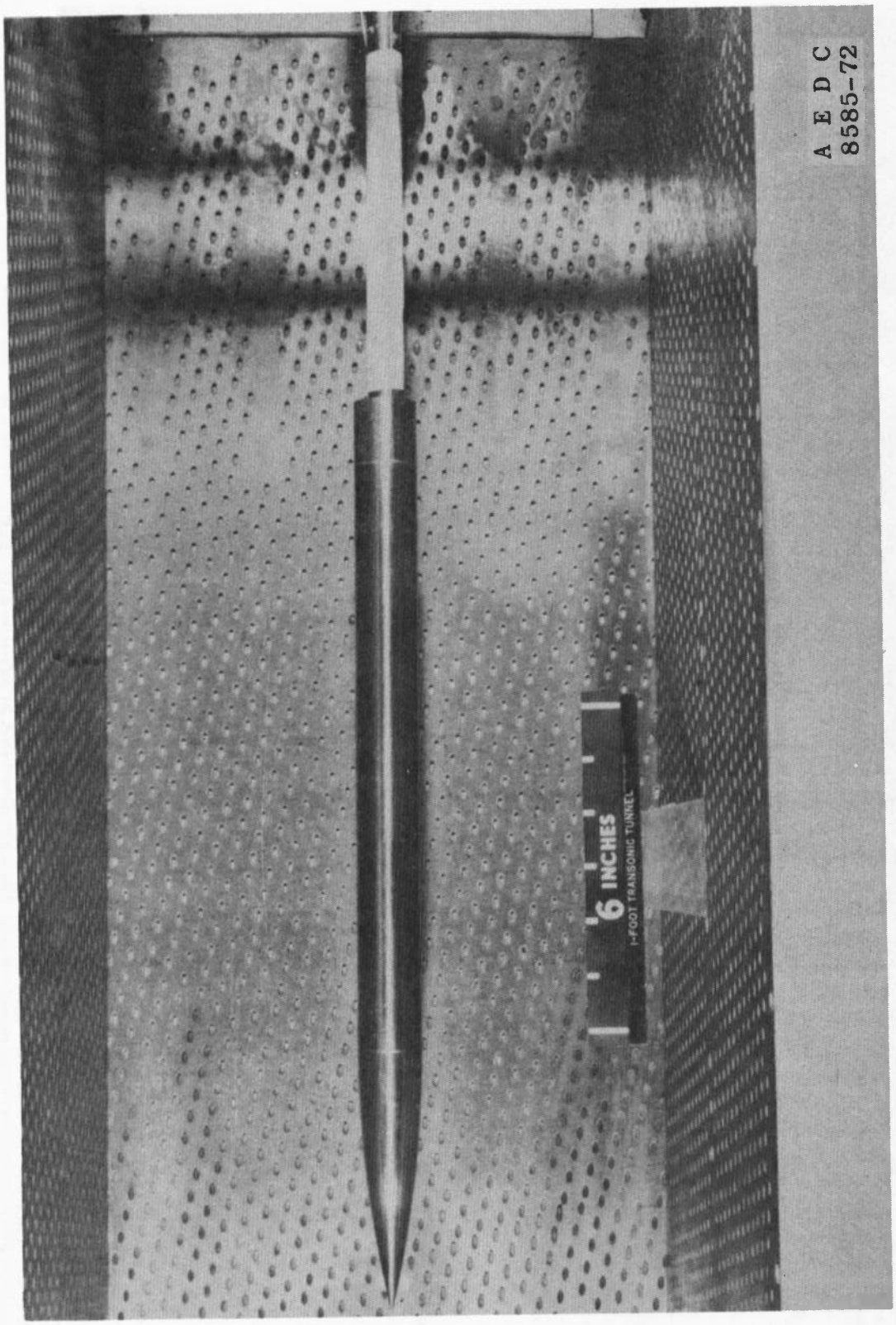

b. N22 M9 A17
Fig. 2 Concluded

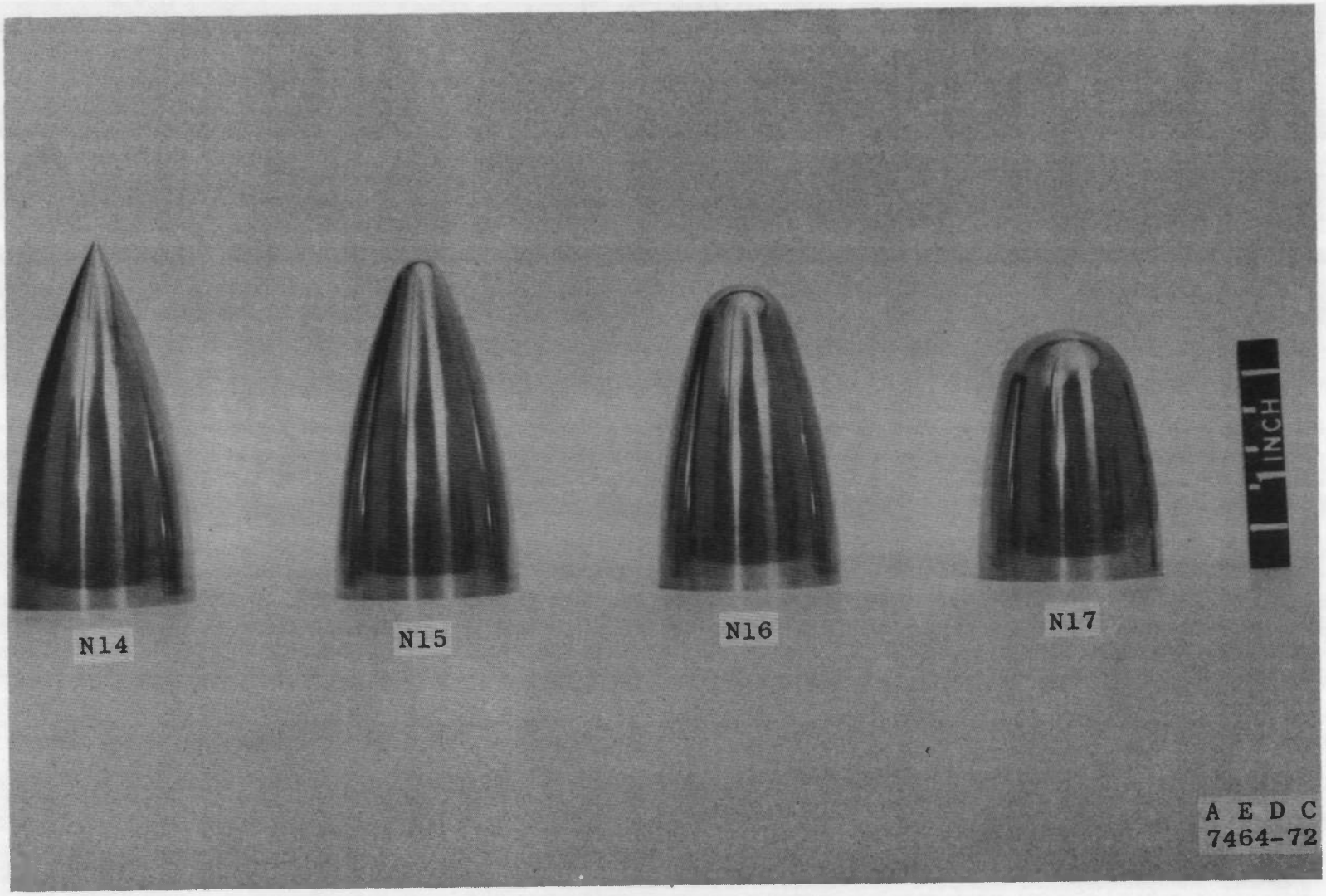

a. 2-cal Tangent Ogive Noses

Fig. 3 Photographs of Model Components

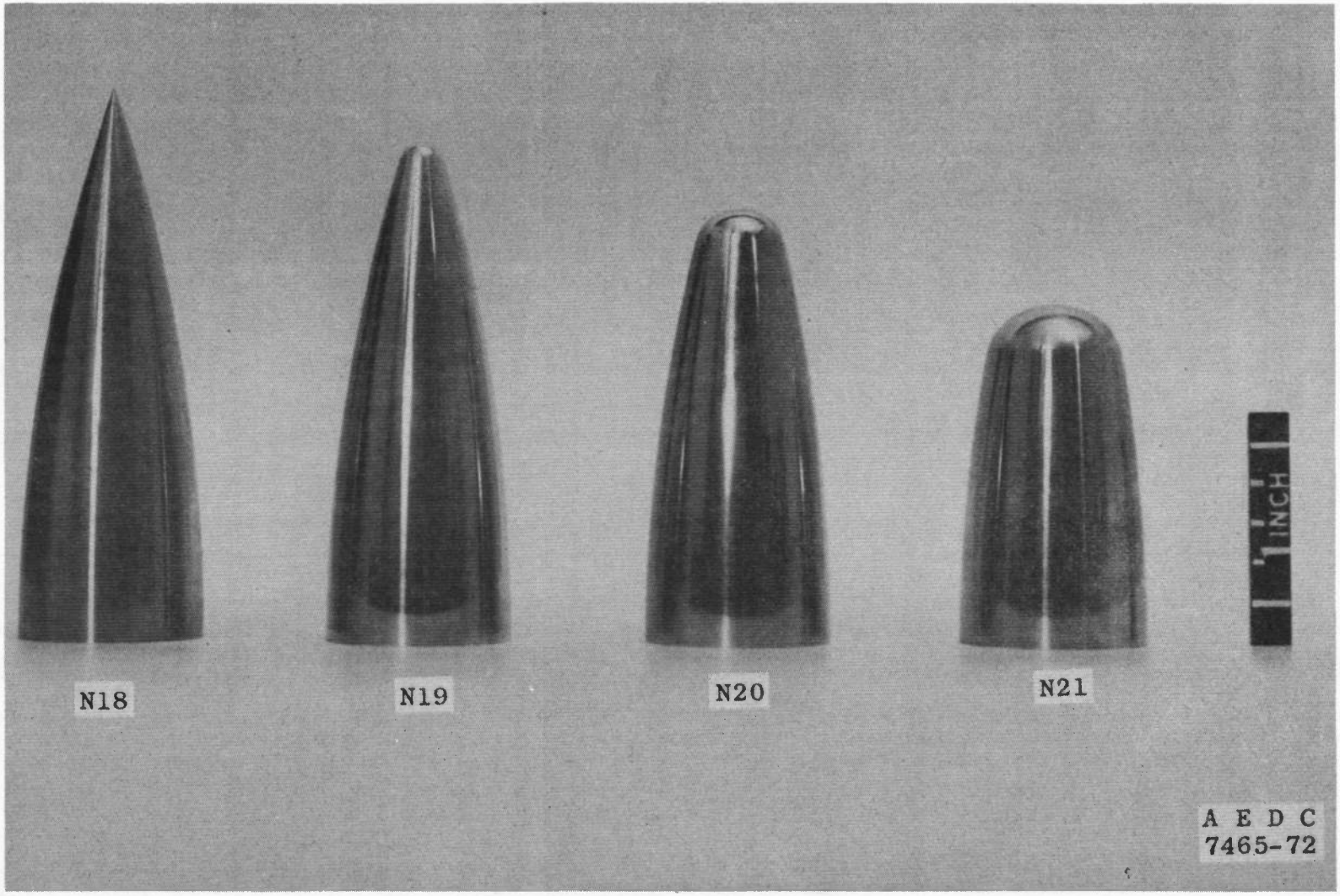

b. 3-cal Tangent Ogive Noses
Fig. 3 Continued

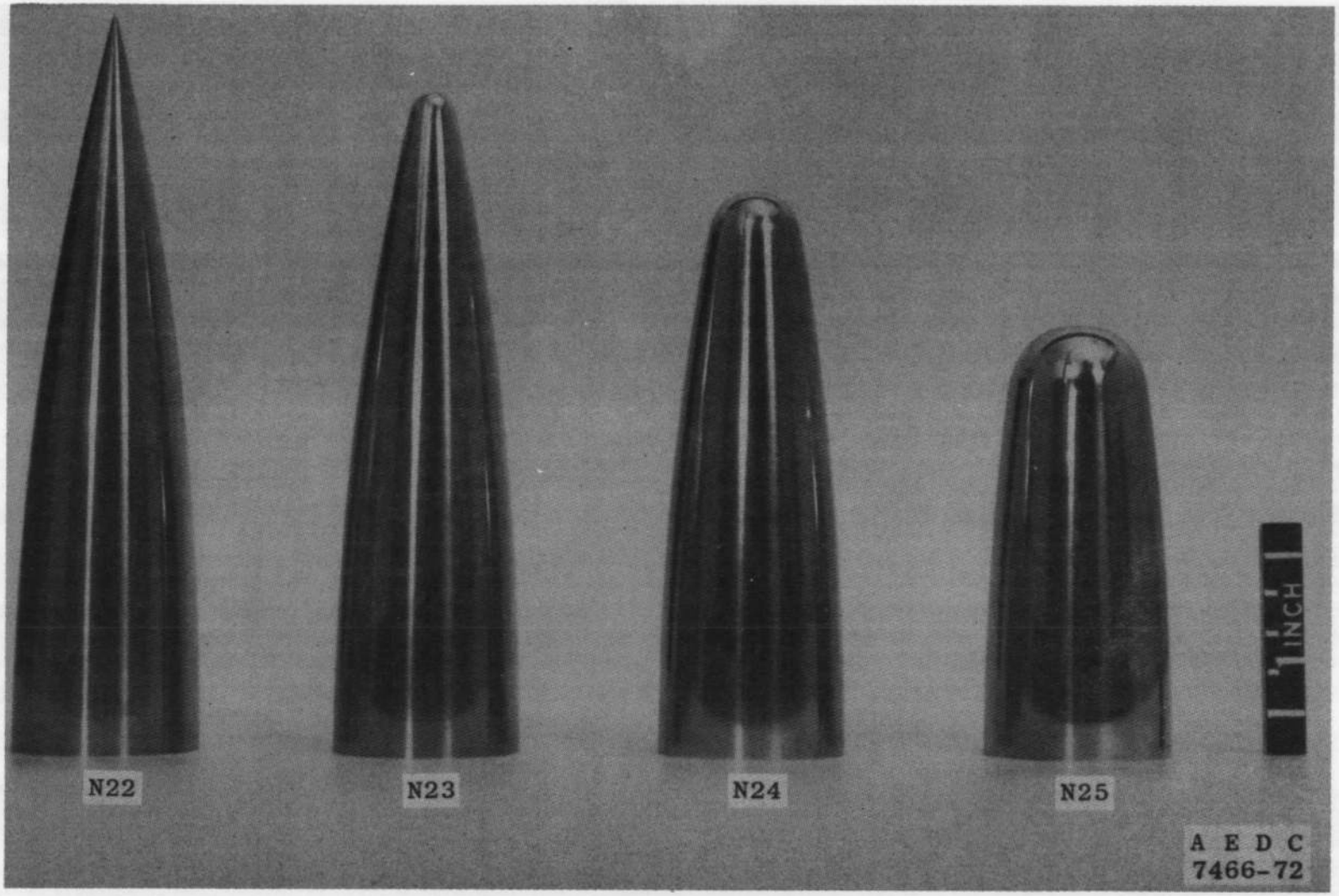

c. 4-cal Tangent Ogive Noses
Fig. 3 Continued

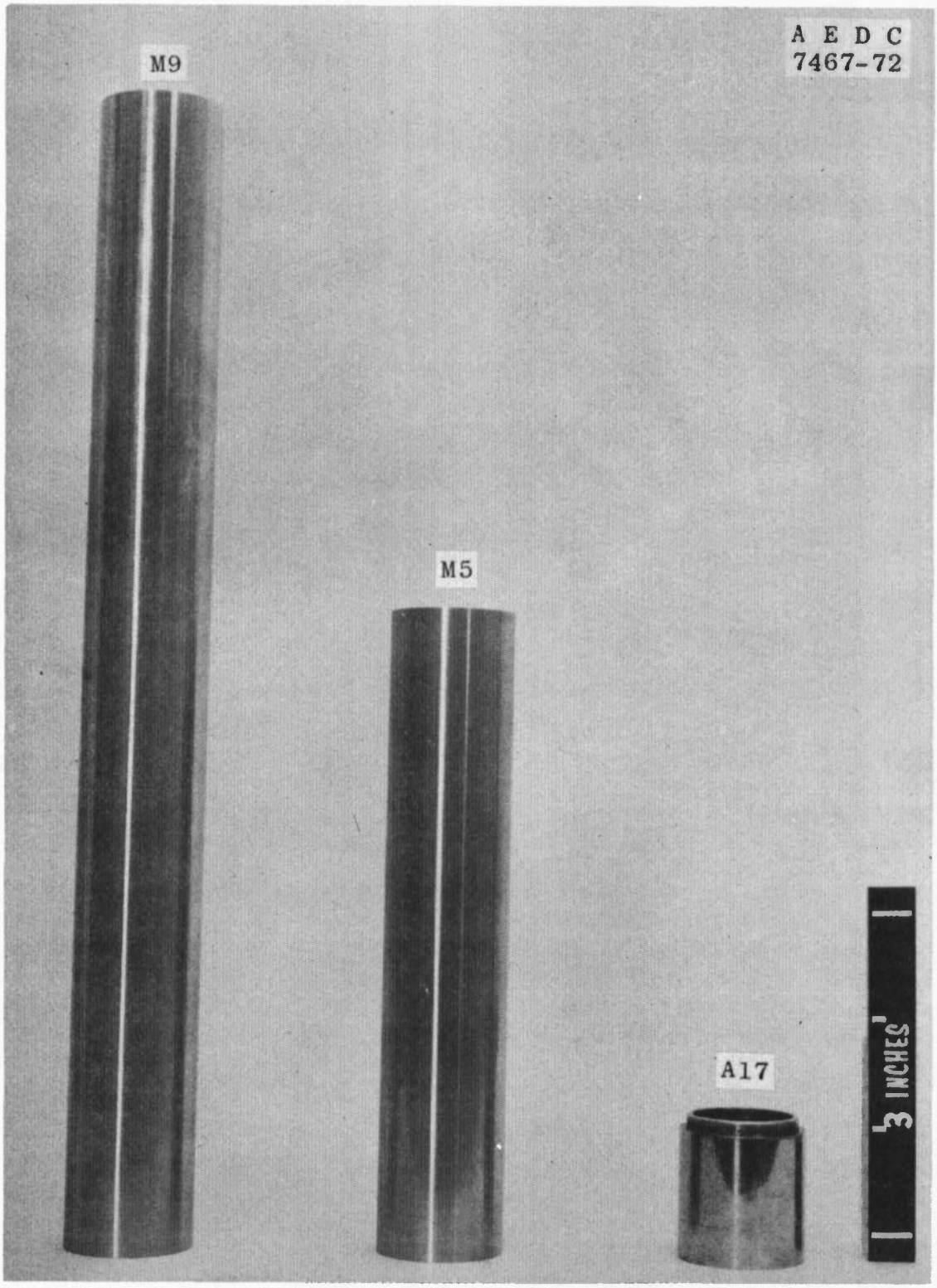

d. M9 and M5 Midbodies, A17 Afterbody
Fig. 3 Concluded

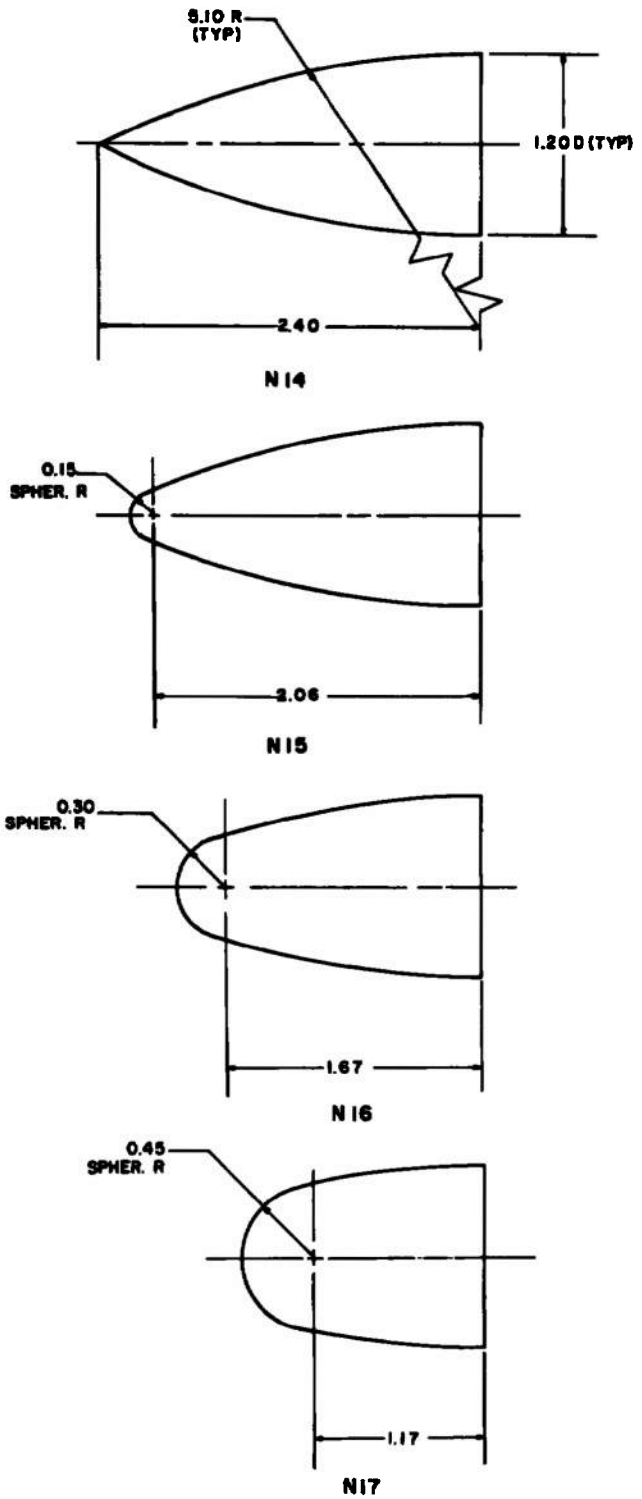

a. 2-cal Tangent Ogive Noses

Fig. 4 Dimensional Sketches of Model Components

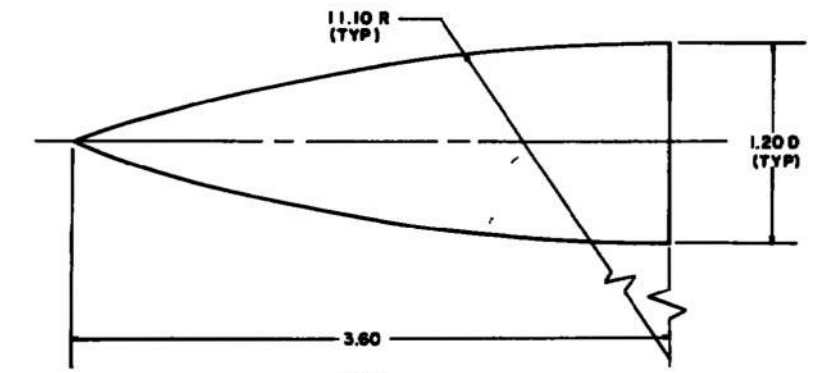

N18

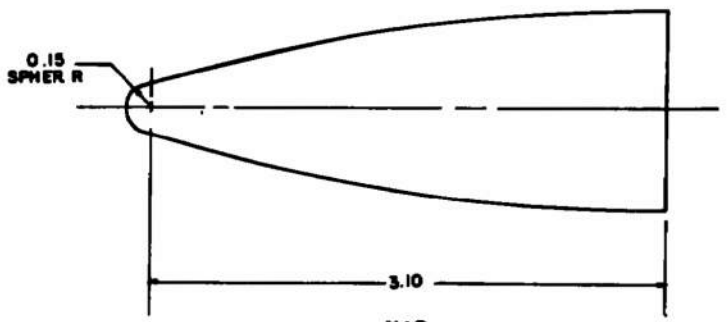

N19

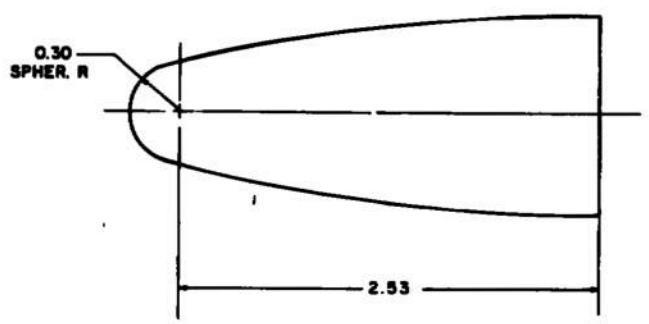

N20

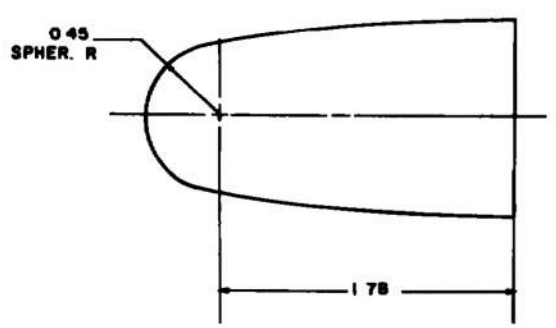

N21

ALL DIMENSIONS IN INCHES

b. 3-cal Tangent Ogive Noses
Fig. 4 Continued

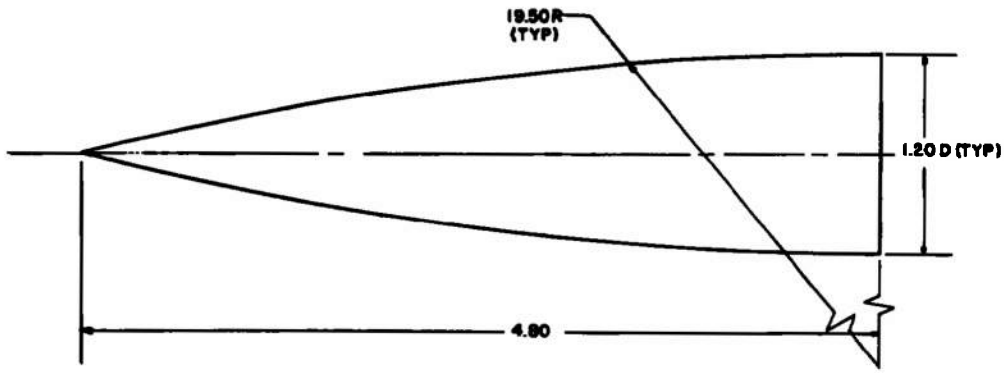

N22

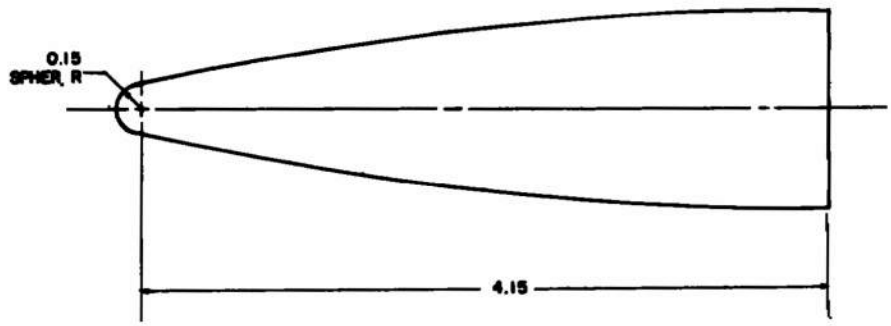

N23

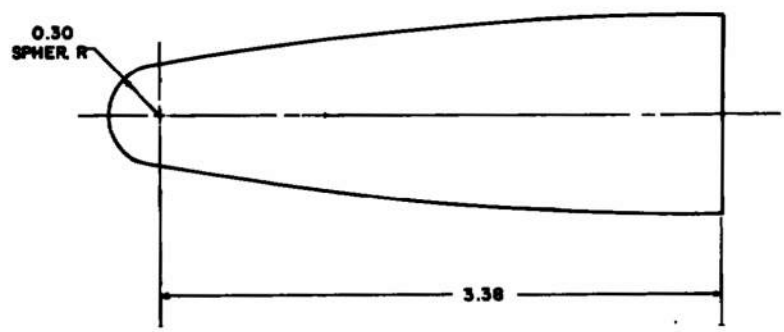

N24

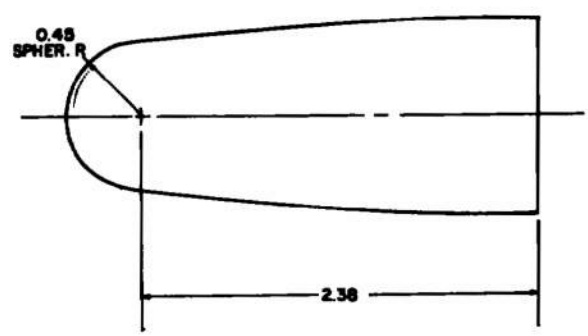

N25

ALL DIMENSIONS IN INCHES

c. 4-cal Tangent Ogive Noses
Fig. 4 Continued

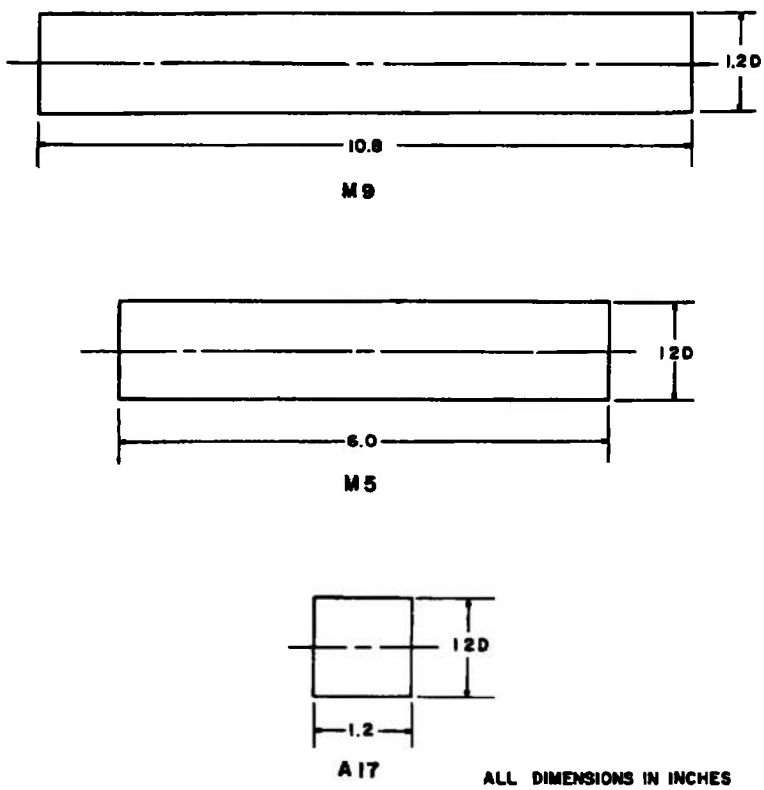

d. M5 and M9 Midbodies, A17 Afterbody
Fig. 4 Concluded

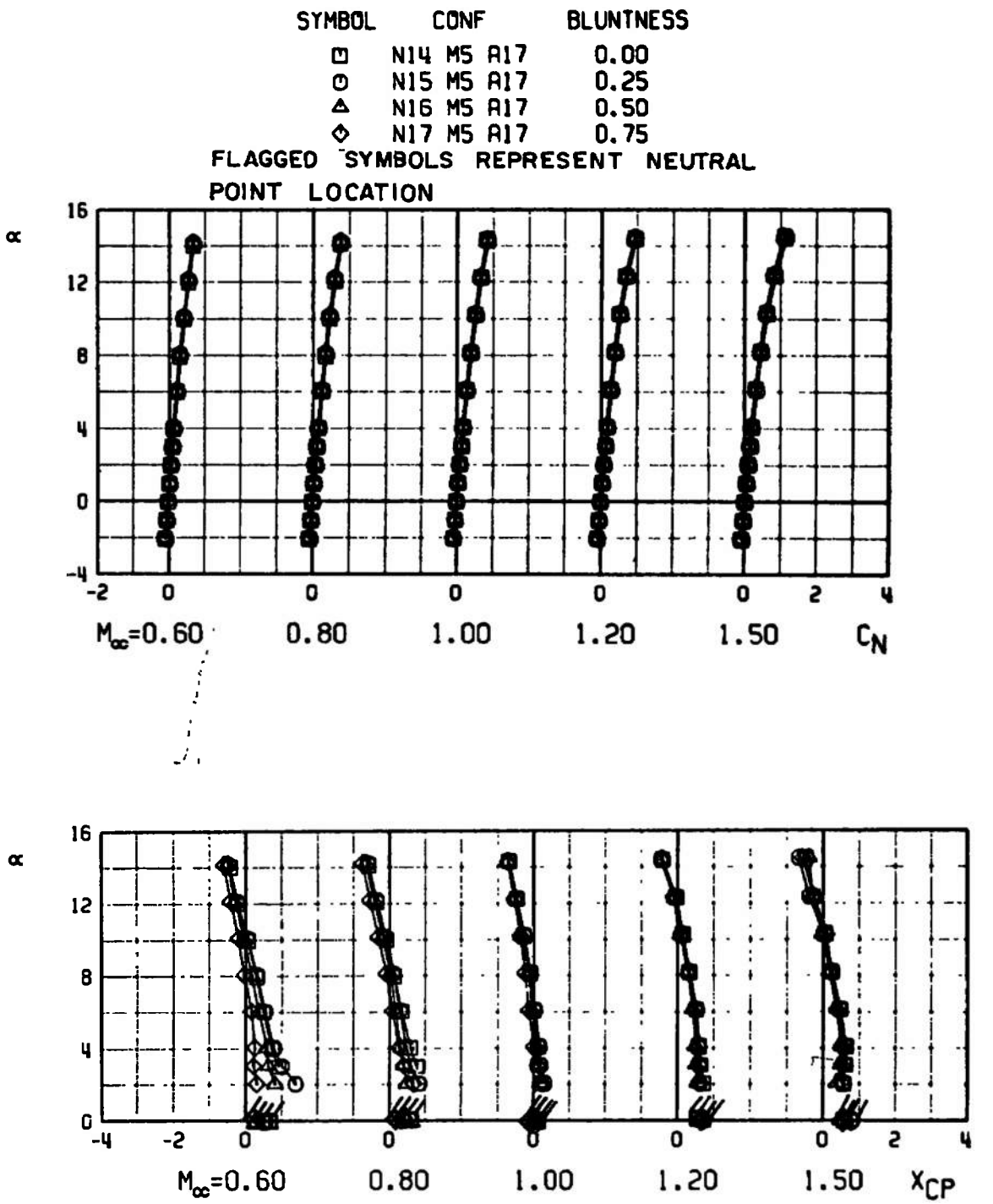

a. Normal-Force Coefficient and Center-of-Pressure Location

Fig. 5 Aerodynamic Coefficients of 2-cal Noses on 5-cal Midbody

SYMBOL	CONF	BLUNTNESS
□	N14 M5 A17	0.00
○	N15 M5 A17	0.25
△	N16 M5 A17	0.50
◇	N17 M5 A17	0.75

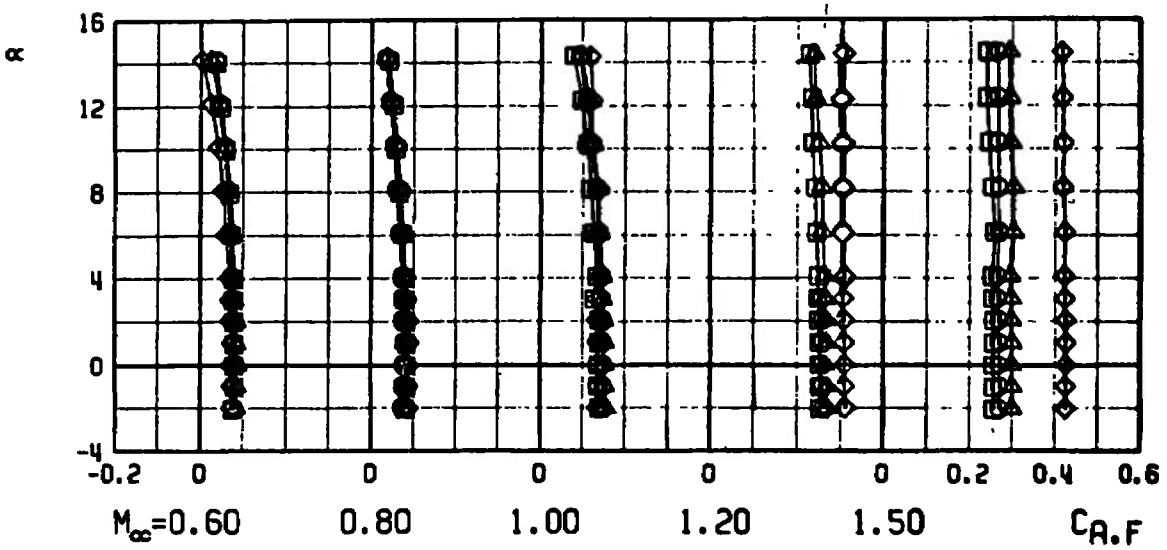

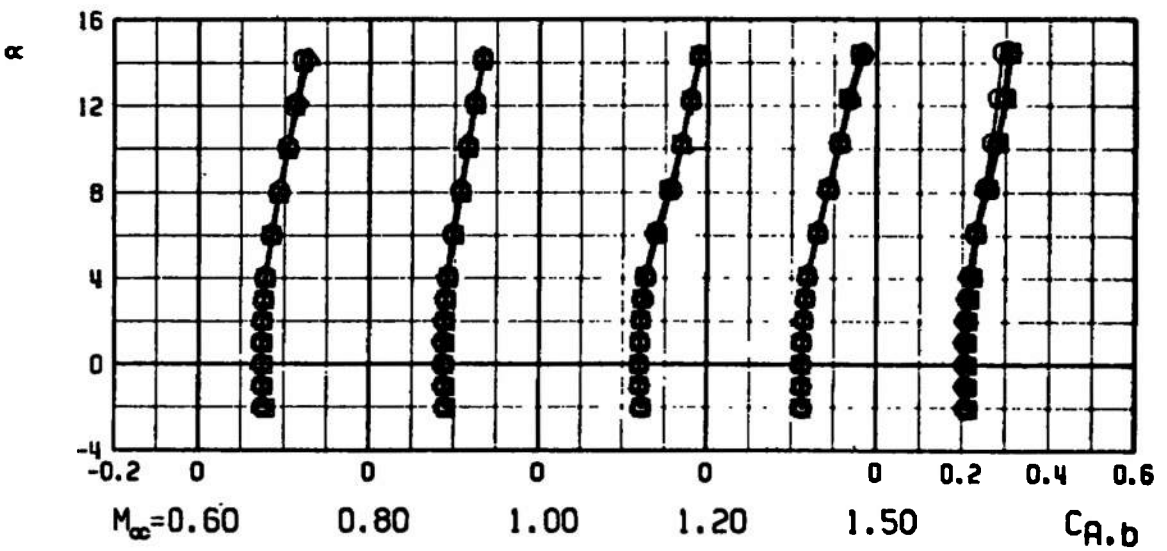

b. Forebody and Base Axial-Force Coefficients
Fig. 5 Concluded

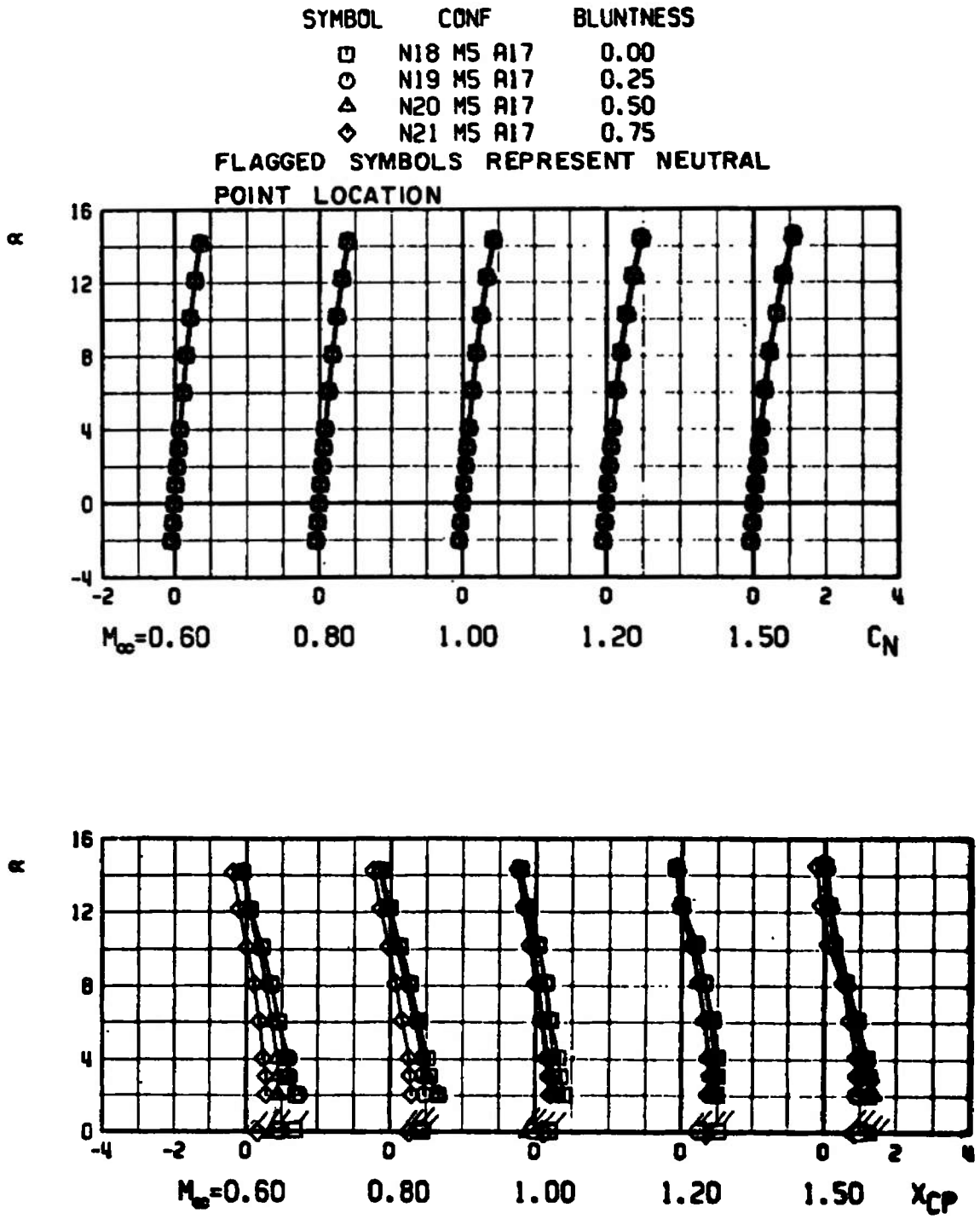

a. Normal-Force Coefficient and Center-of-Pressure Location

Fig. 6 Aerodynamic Coefficients of 3-cal Noses on 5-cal Midbody

SYMBOL	CONF	BLUNTNESS
□	N18 M5 A17	0.00
○	N19 M5 A17	0.25
△	N20 M5 A17	0.50
◇	N21 M5 A17	0.75

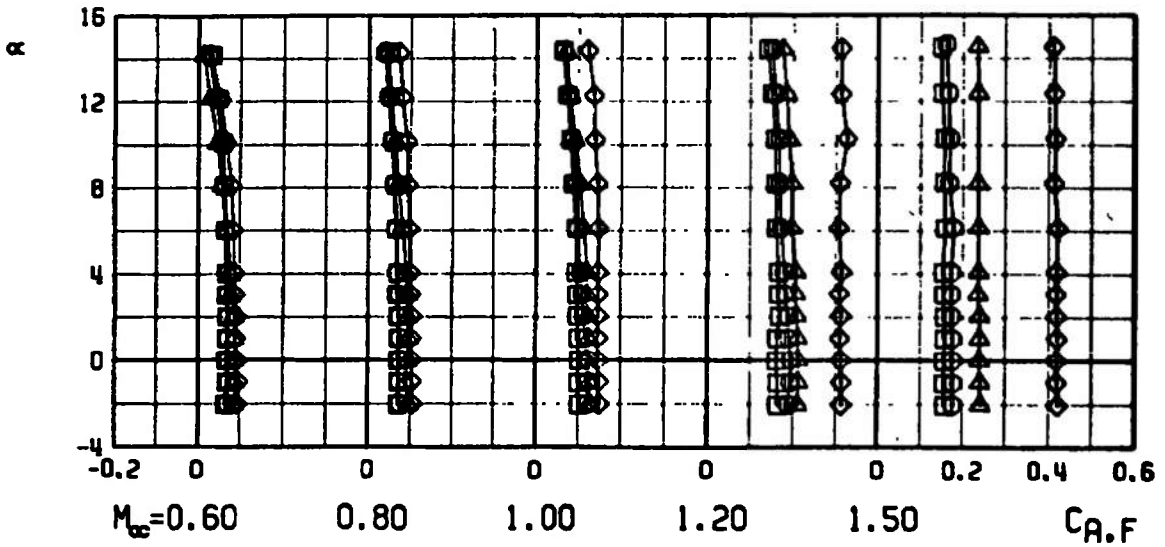

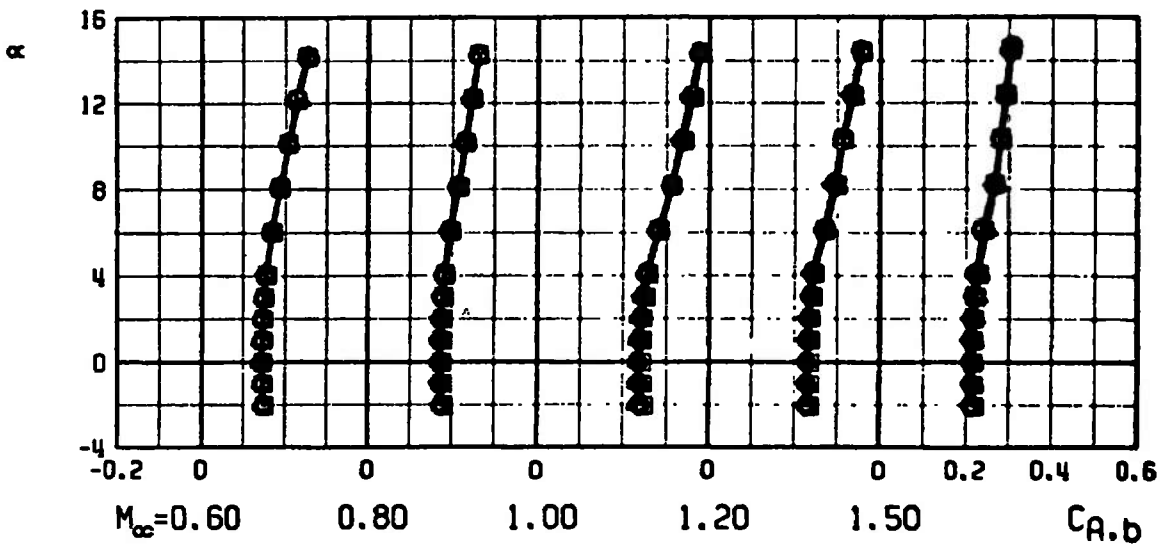

b. Forebody and Base Axial-Force Coefficients
Fig. 6 Concluded

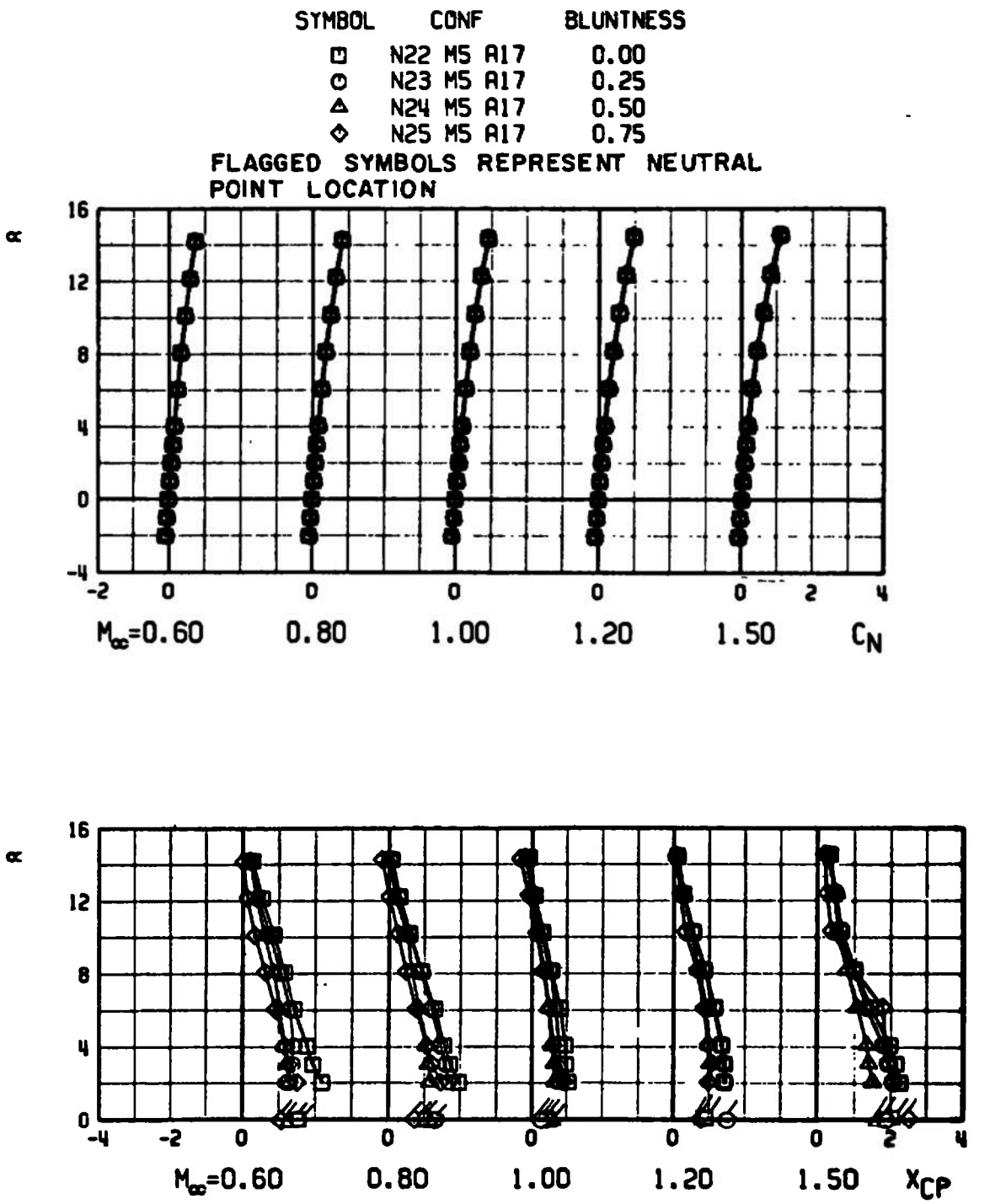

a. Normal-Force Coefficient and Center-of-Pressure Location

Fig. 7 Aerodynamic Coefficients of 4-cal Noses on 5-cal Midbody

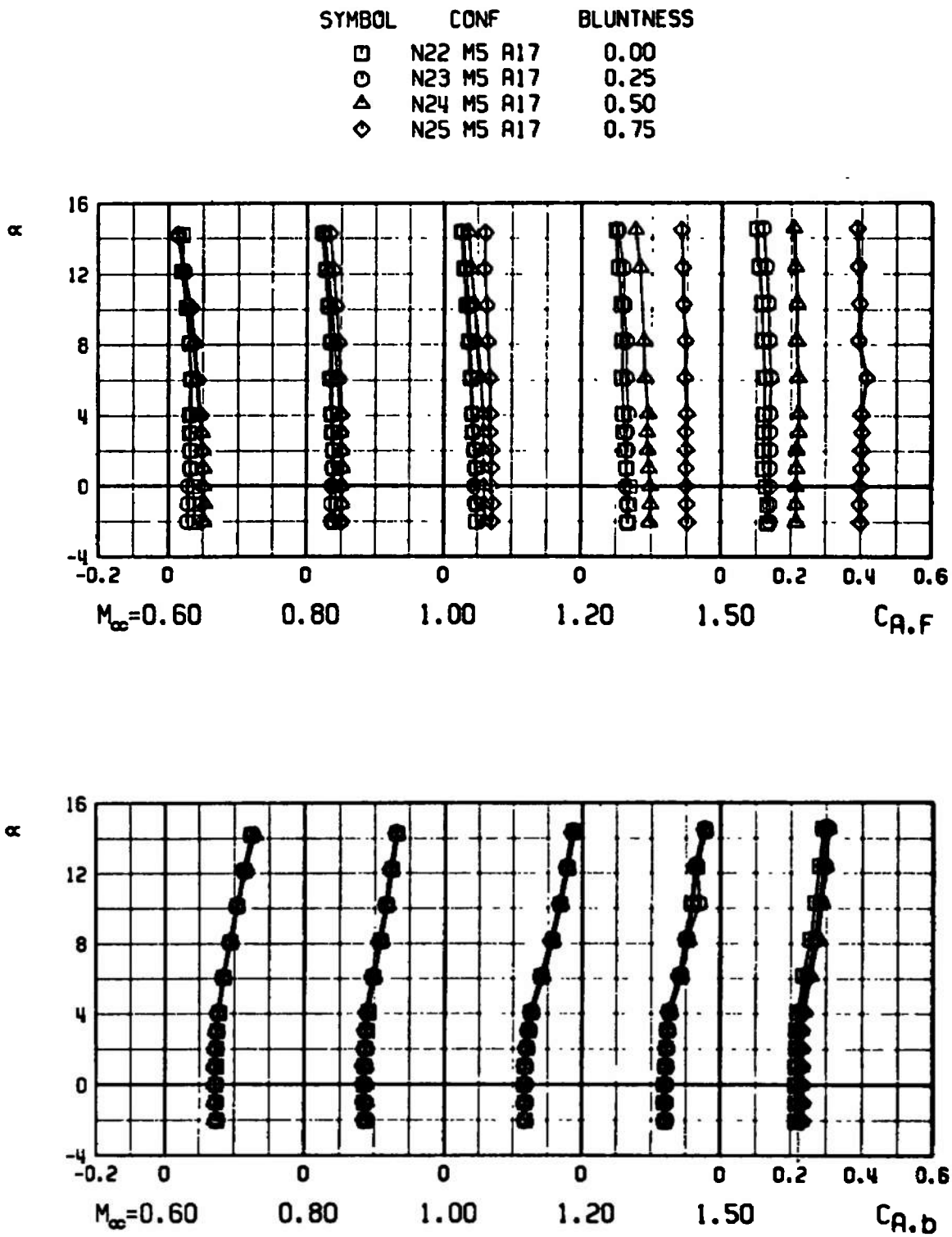

b. Forebody and Base Axial-Force Coefficients
Fig. 7 Concluded

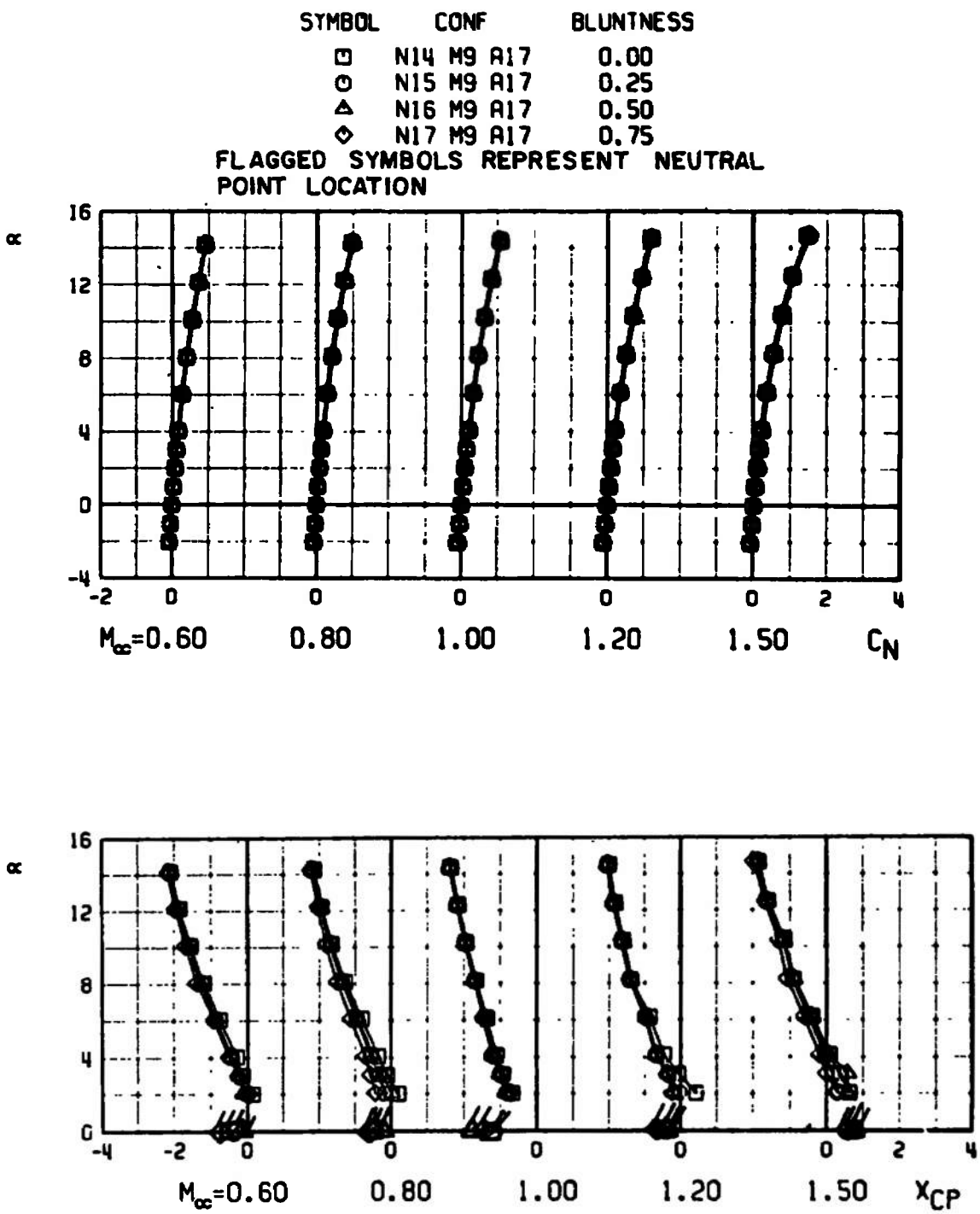

a. Normal-Force Coefficient and Center-of-Pressure Location

Fig. 8 Aerodynamic Coefficients of 2-cal Noses on 9-cal Midbody

SYMBOL	CONF	BLUNTNESS
□	N14 M9 A17	0.00
○	N15 M9 A17	0.25
△	N16 M9 A17	0.50
◇	N17 M9 A17	0.75

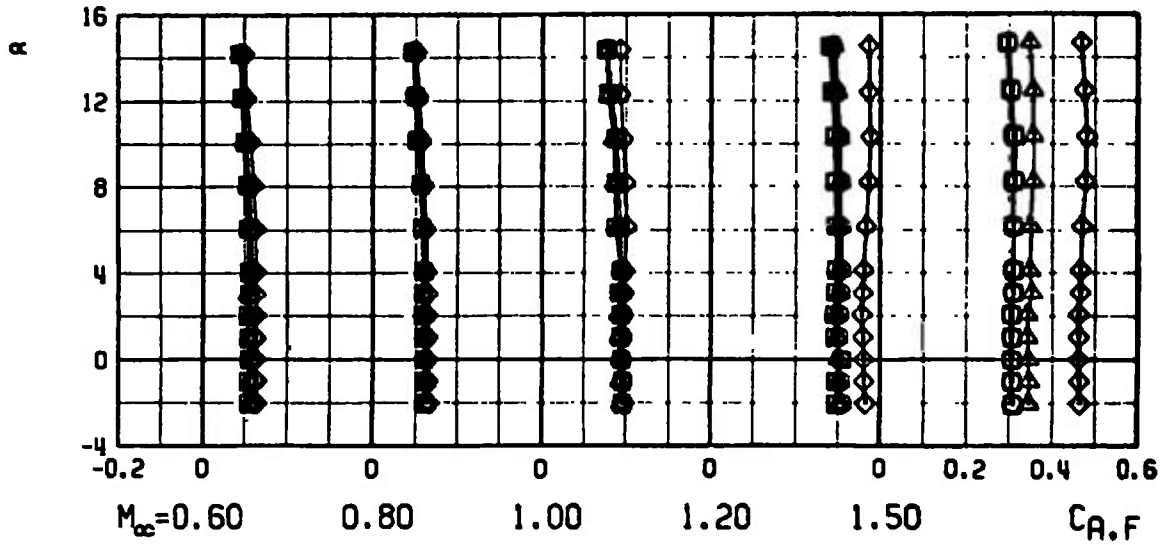

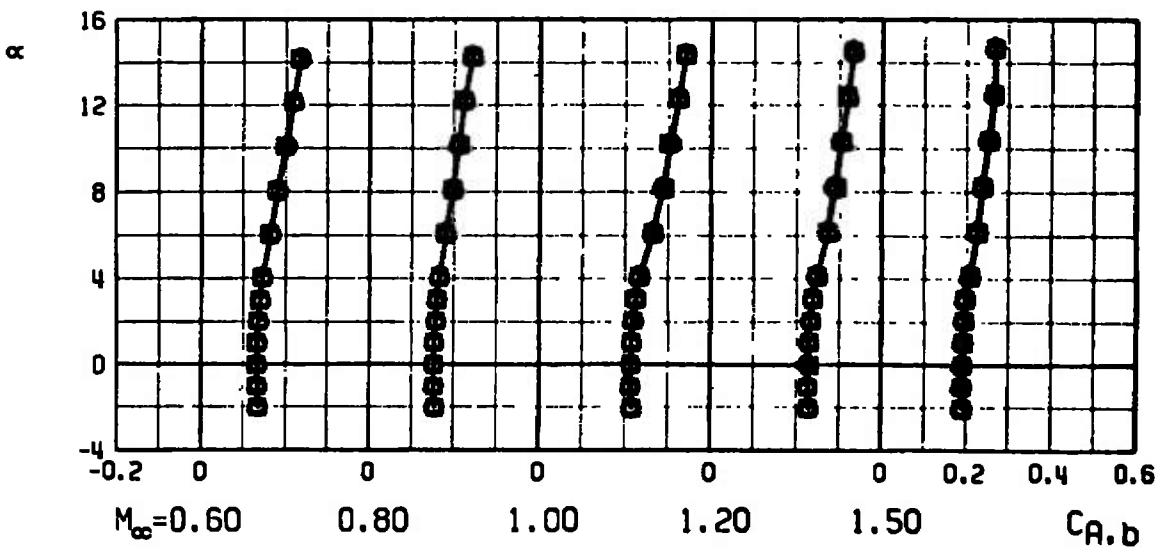

b. Forebody and Base Axial-Force Coefficients
Fig. 8 Concluded

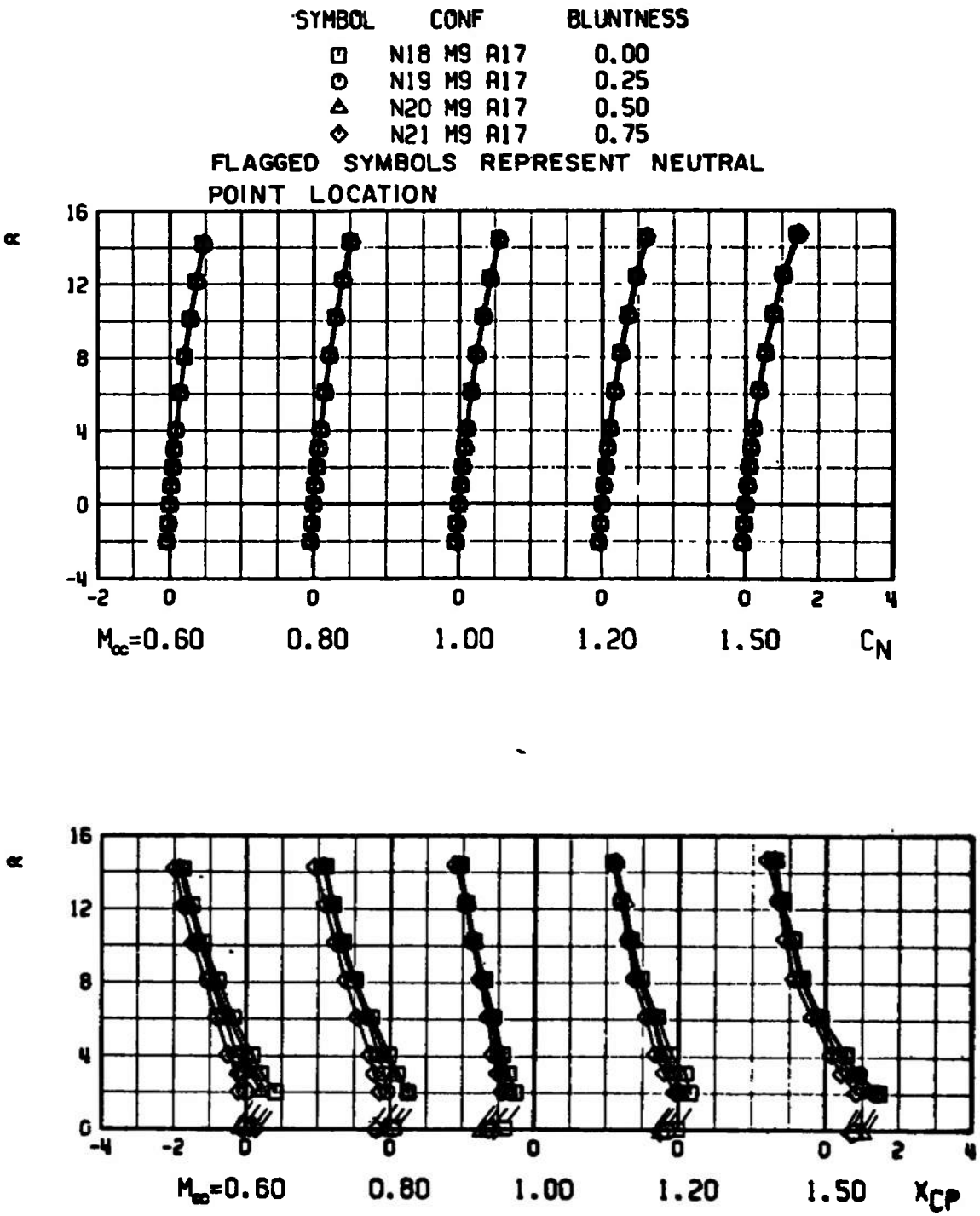

a. Normal-Force Coefficient and Center-of-Pressure Location

Fig. 9 Aerodynamic Coefficients of 3-cal Noses on 9-cal Midbody

SYMBOL	CONF	BLUNTNESS
□	N18 M9 A17	0.00
○	N19 M9 A17	0.25
△	N20 M9 A17	0.50
◇	N21 M9 A17	0.75

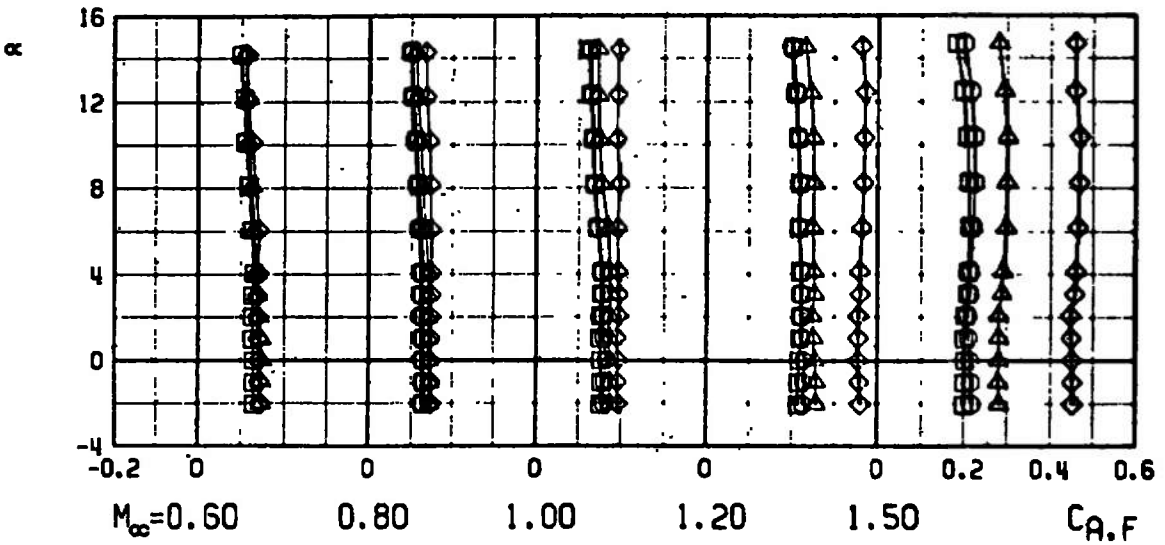

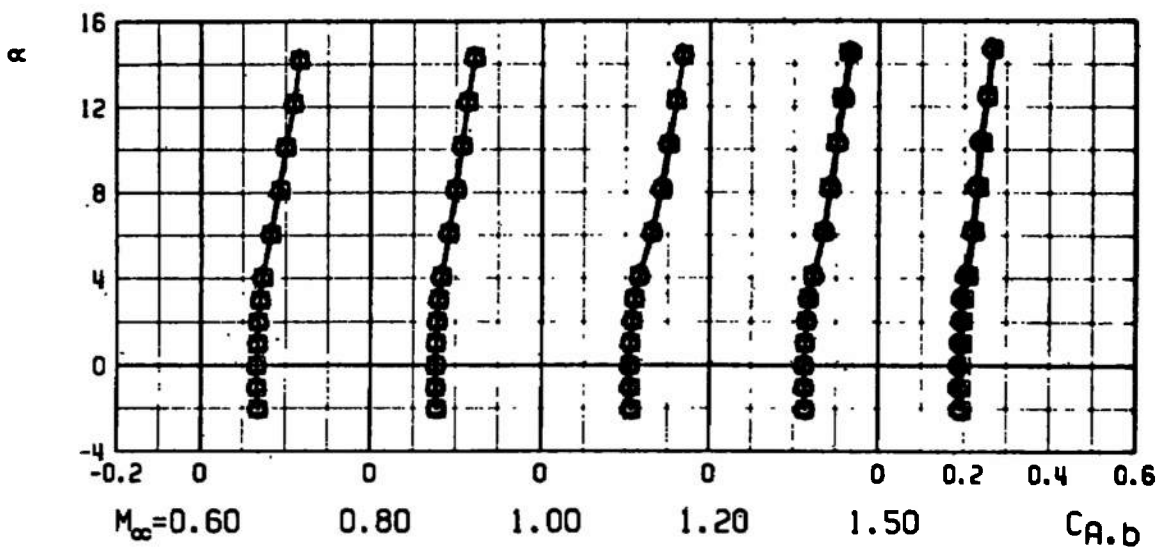

b. Forebody and Base Axial-Force Coefficients
Fig. 9 Concluded

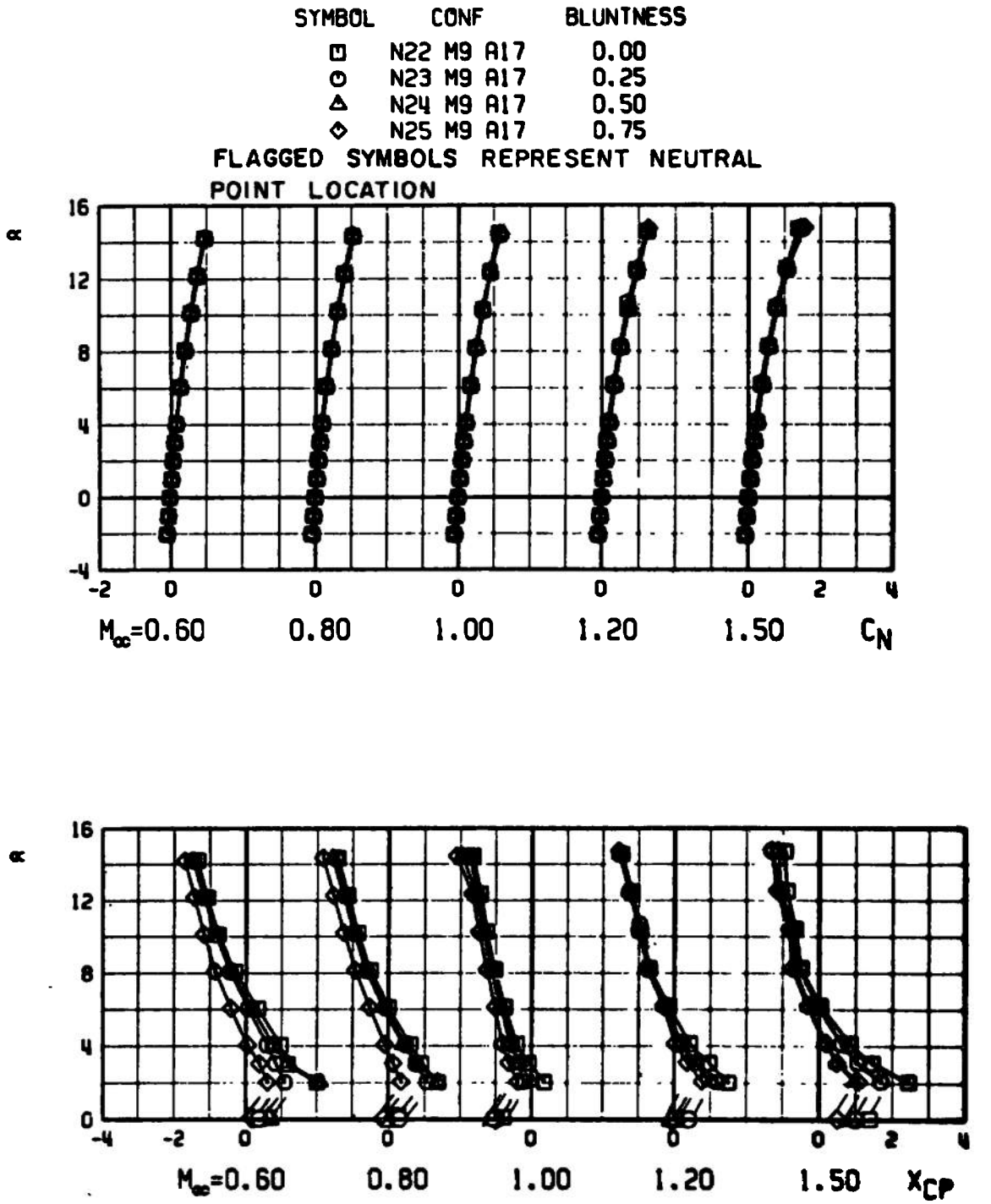

a. Normal-Force Coefficient and Center-of-Pressure Location

Fig. 10 Aerodynamic Coefficients of 4-cal Noses on 9-cal Midbody

SYMBOL	CONF	BLUNTNESS
□	N22 M9 A17	0.00
○	N23 M9 A17	0.25
△	N24 M9 A17	0.50
◇	N25 M9 A17	0.75

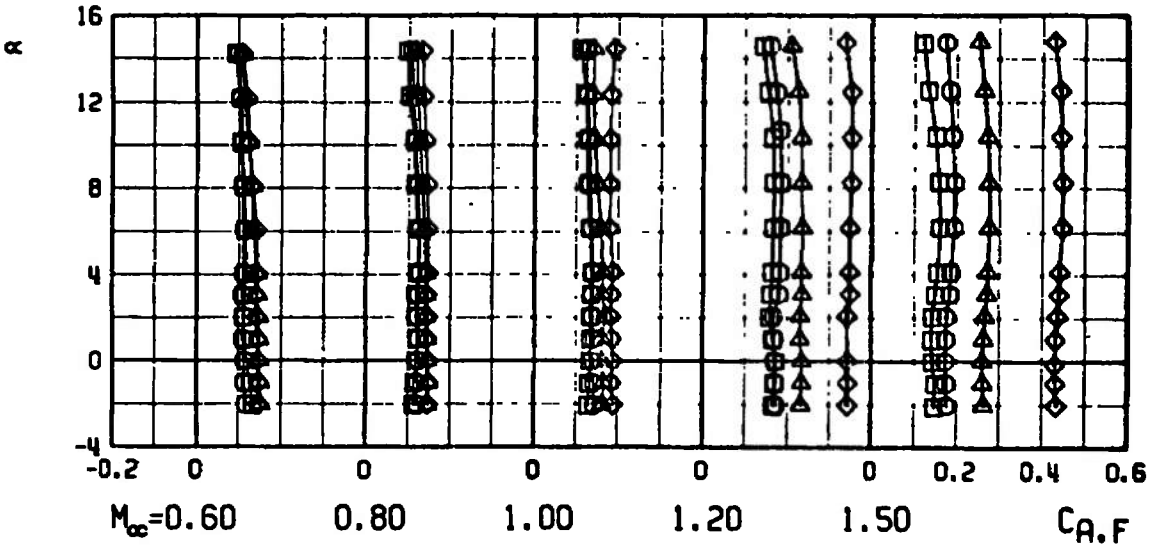

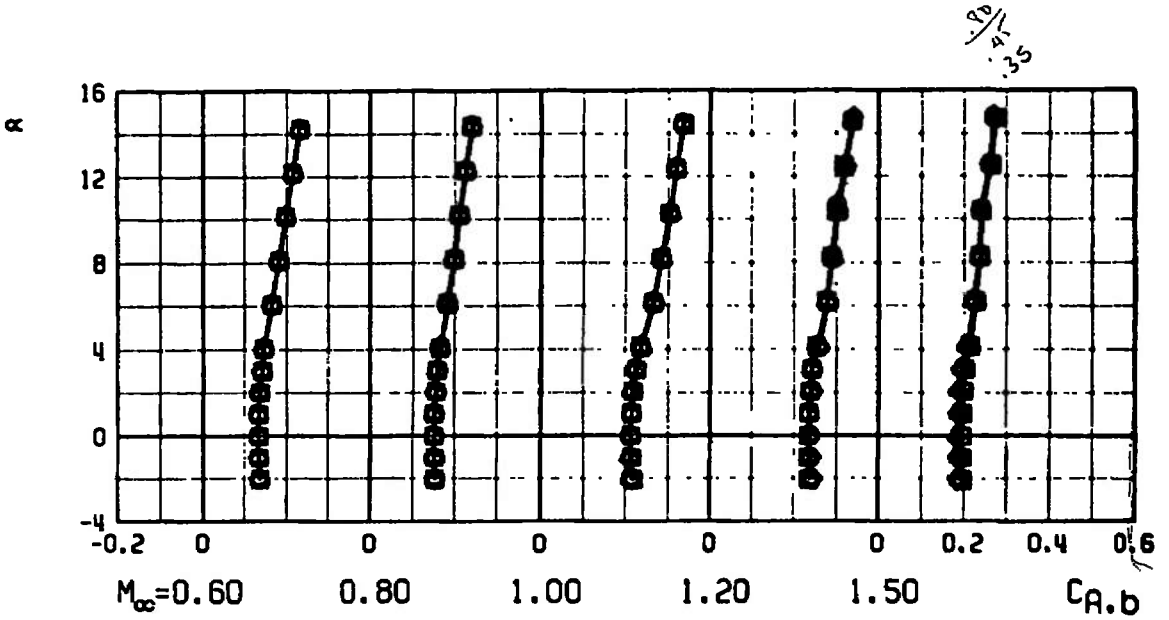

b. Forebody and Base Axial-Force Coefficients
Fig. 10 Concluded

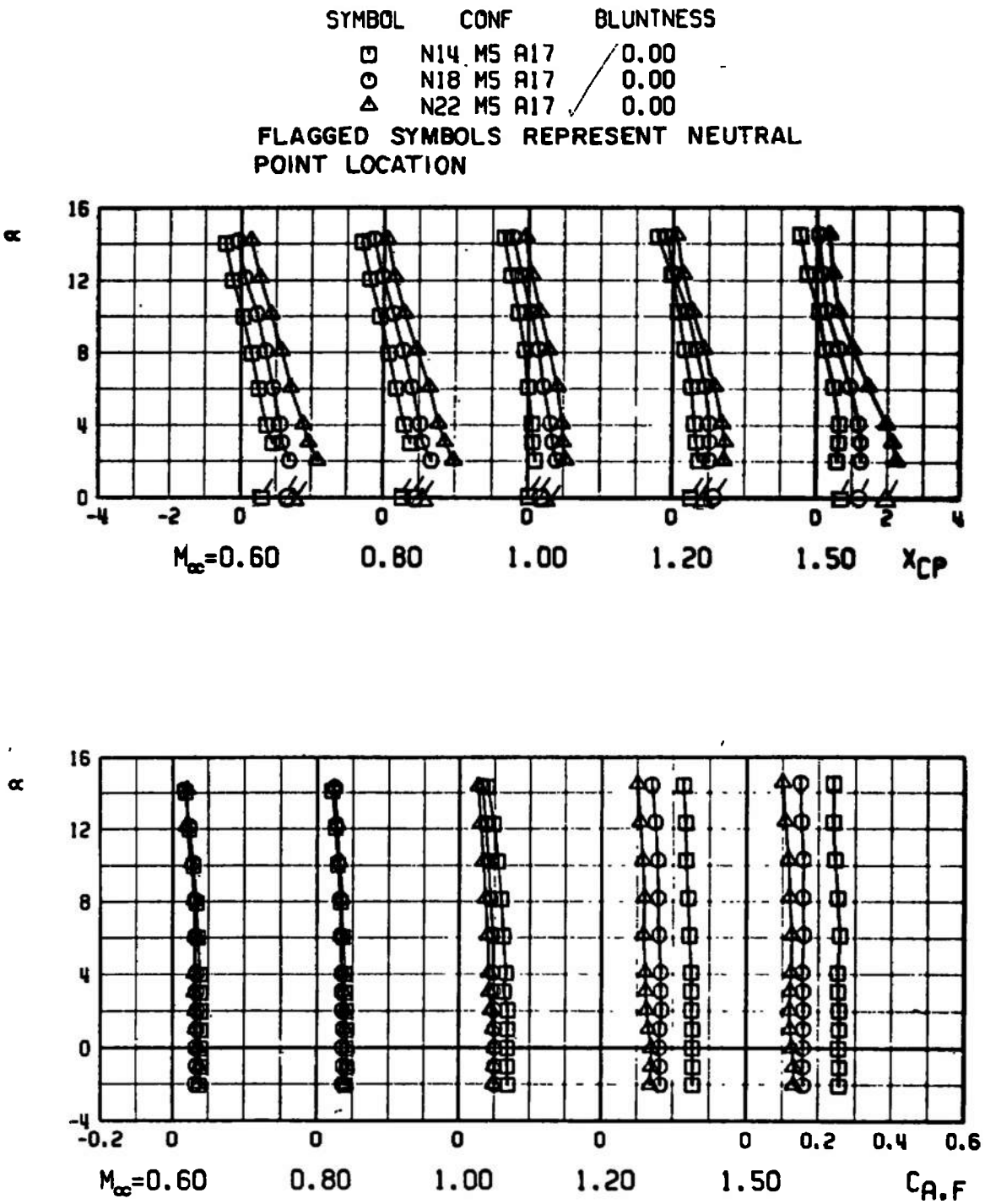

a. Zero Bluntness Ratio

Fig. 11 Comparison of Center-of-Pressure Location and Forebody Axial-Force Coefficients of Noses on 5-cal Midbody

SYMBOL	CONF	BLUNTNESS
□	N15 M5 A17	0.25
○	N19 M5 A17	0.25
△	N23 M5 A17	0.25

FLAGGED SYMBOLS REPRESENT NEUTRAL POINT LOCATION

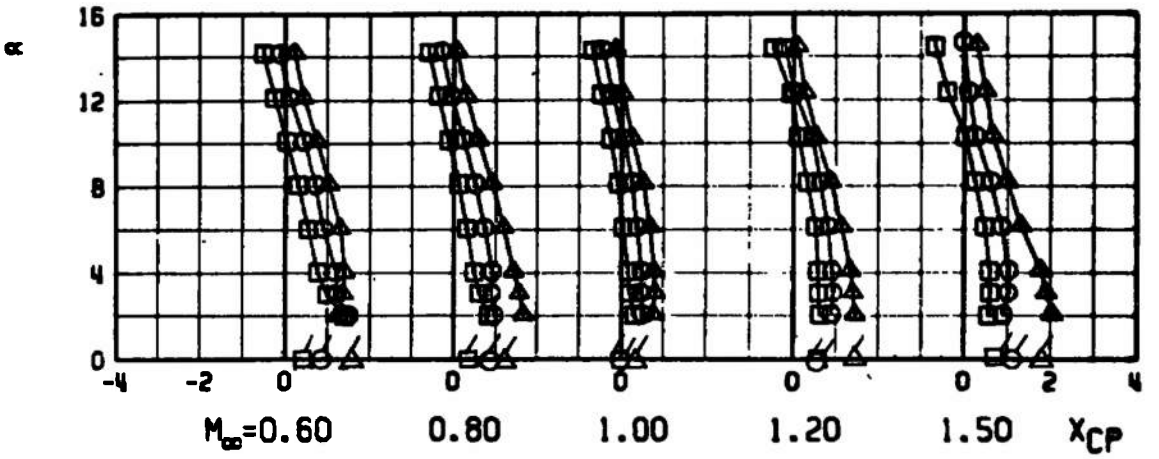

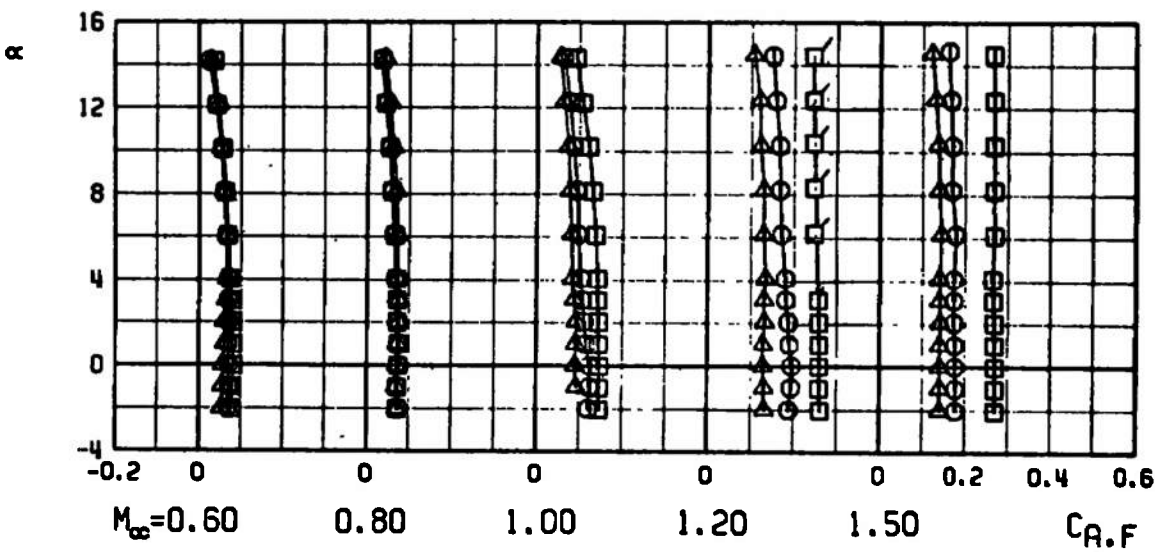

b. 0.25 Bluntness Ratio
Fig. 11 Continued

SYMBOL	CONF	BLUNTNESS
□	N16 M5 A17	0.50
○	N20 M5 A17	0.50
△	N24 M5 A17	0.50

FLAGGED SYMBOLS REPRESENT NEUTRAL POINT LOCATION

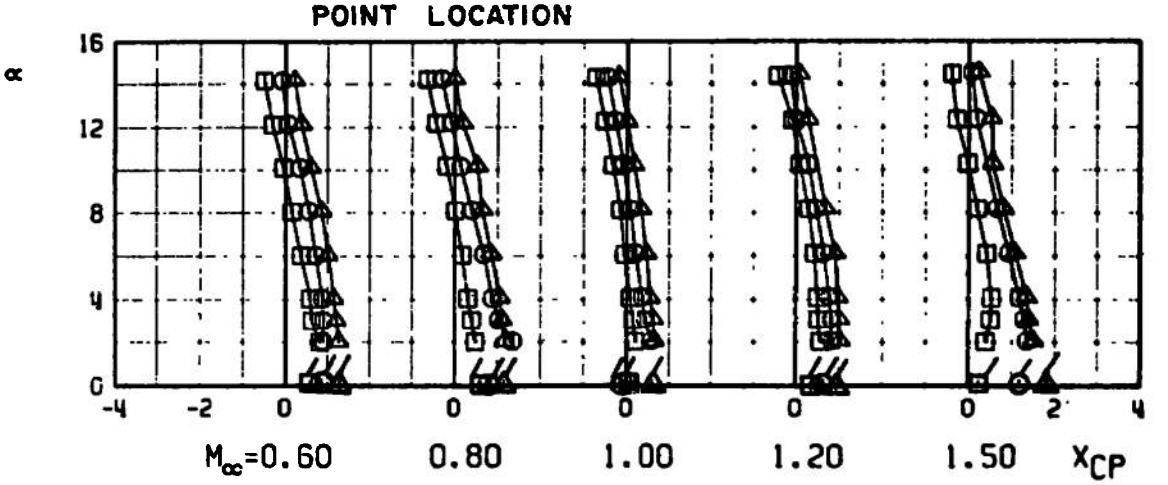

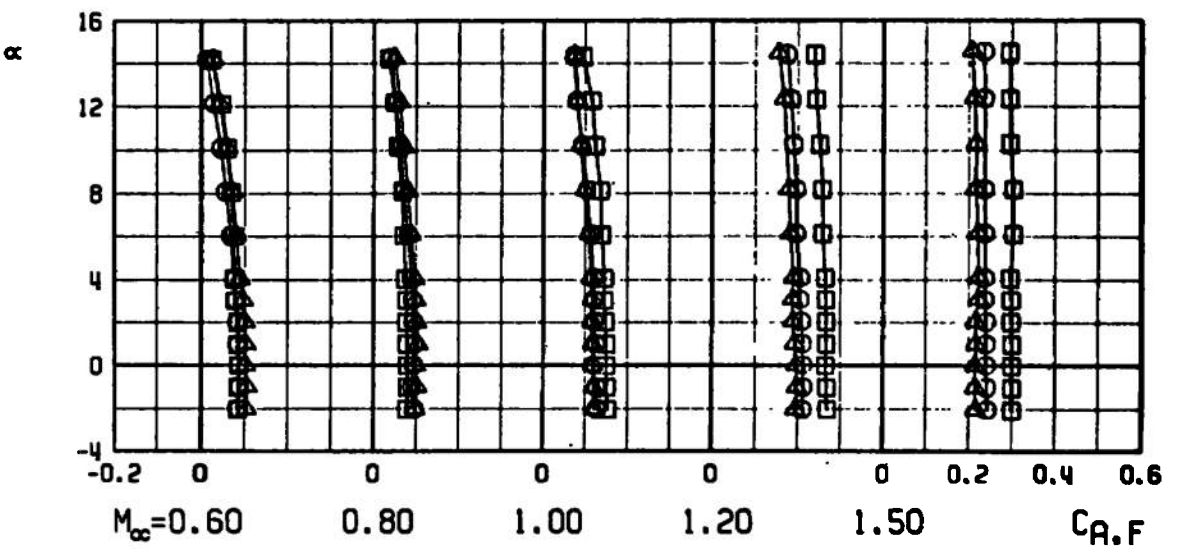

c. 0.50 Bluntness Ratio
Fig. 11 Continued

SYMBOL	CONF	BLUNTNESS
□	N17 M5 A17	0.75
○	N21 M5 A17	0.75
△	N25 M5 A17	0.75

FLAGGED SYMBOLS REPRESENT NEUTRAL POINT LOCATION

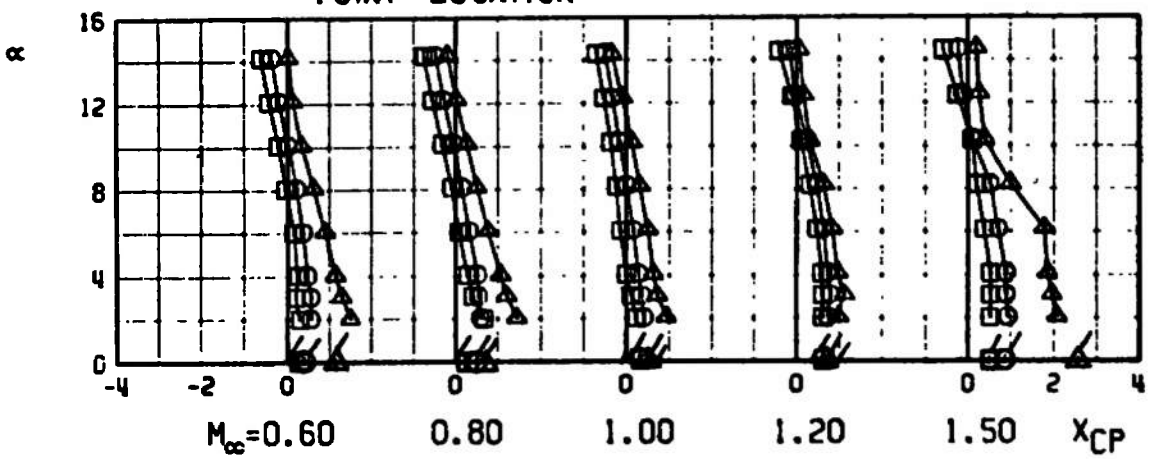

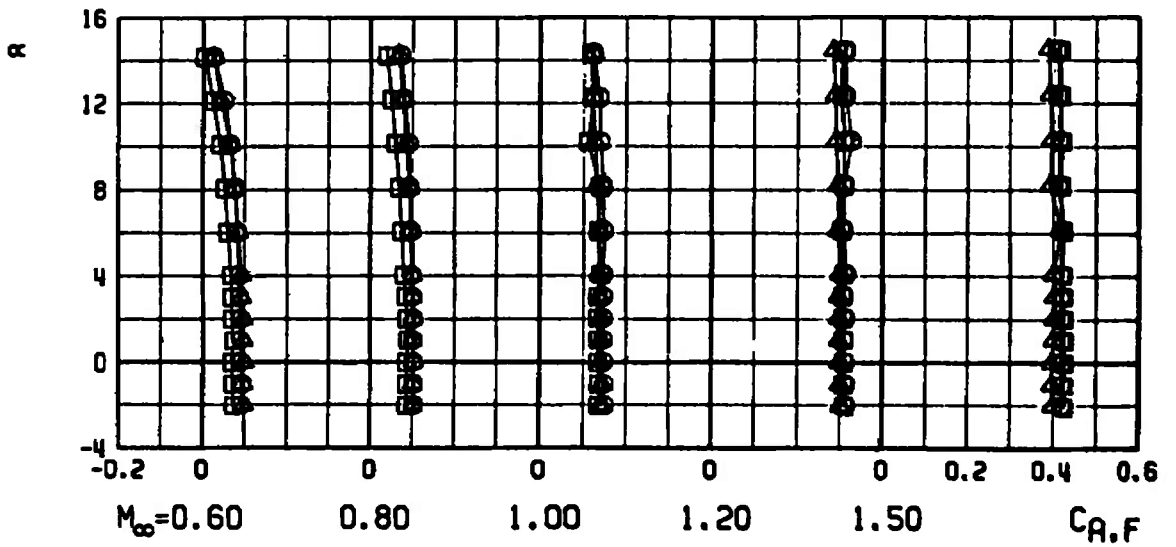

d. 0.75 Bluntness Ratio
Fig. 11 Concluded

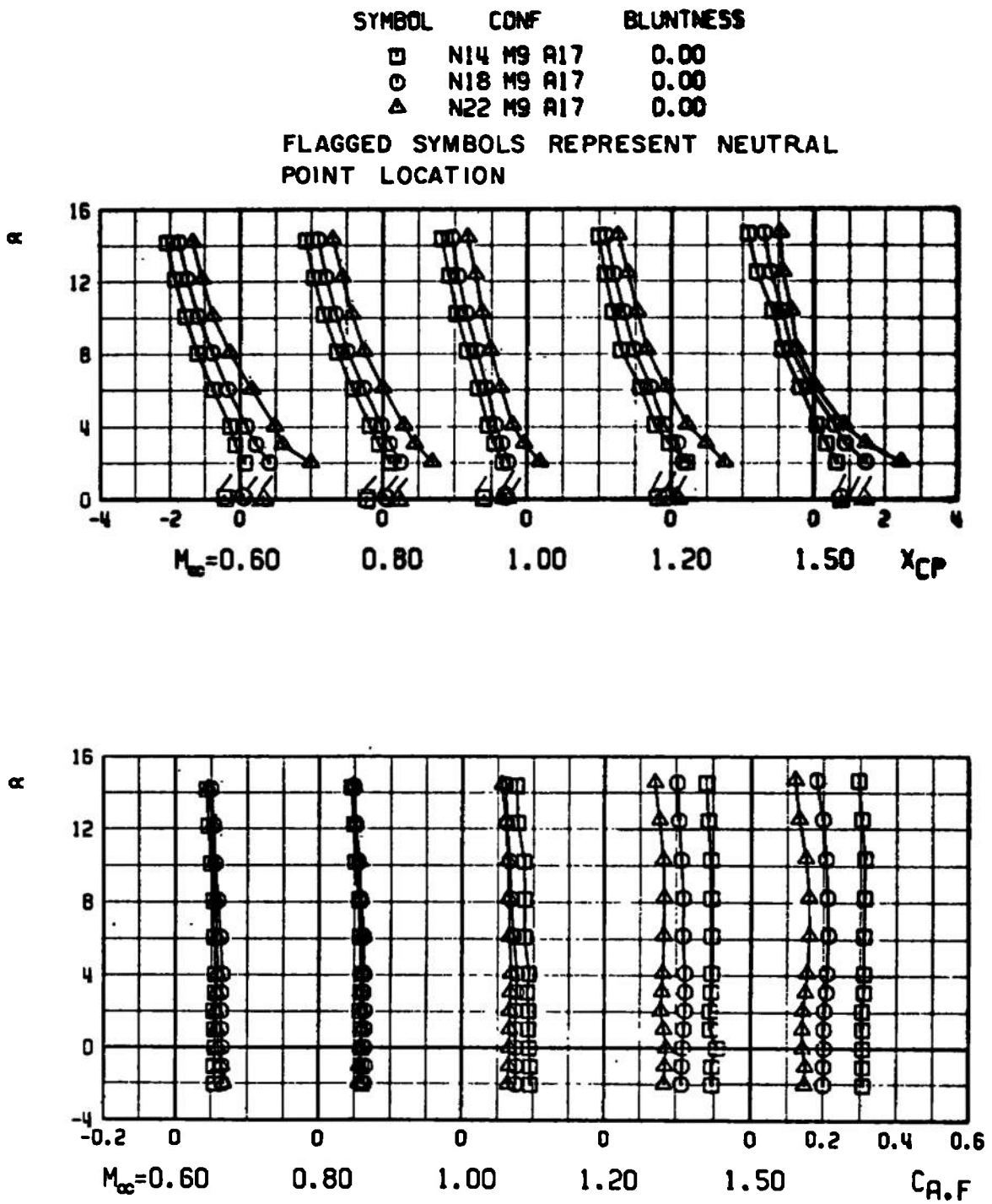

a. Zero Bluntness Ratio

Fig. 12 Comparison of Center-of-Pressure Location and Forebody Axial-Force Coefficients of Noses on 9-cal Midbody

SYMBOL	CONF	BLUNTNESS
□	N15 M9 A17	0.25
○	N19 M9 A17	0.25
△	N23 M9 A17	0.25

FLAGGED SYMBOLS REPRESENT NEUTRAL POINT LOCATION

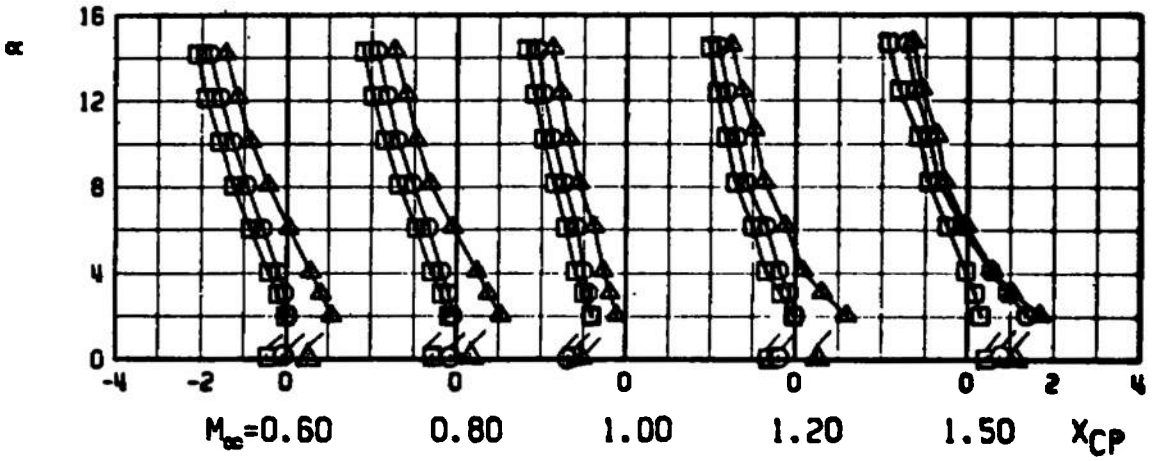

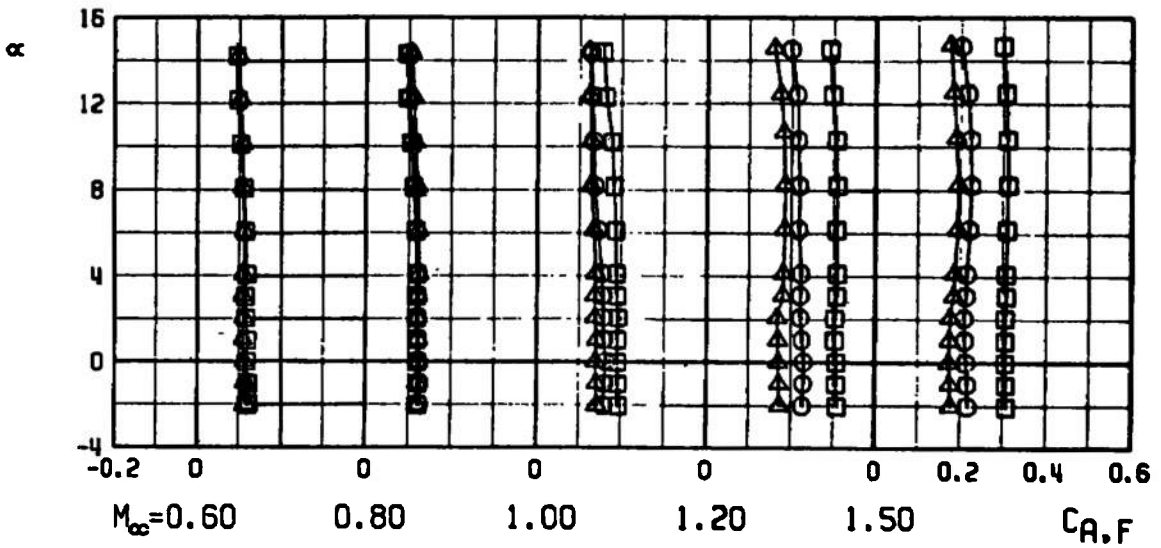

b. 0.25 Bluntness Ratio
Fig. 12 Continued

SYMBOL	CONF	BLUNTNESS
□	N16 M9 A17	0.50
○	N20 M9 A17	0.50
△	N24 M9 A17	0.50

FLAGGED SYMBOLS REPRESENT NEUTRAL POINT LOCATION

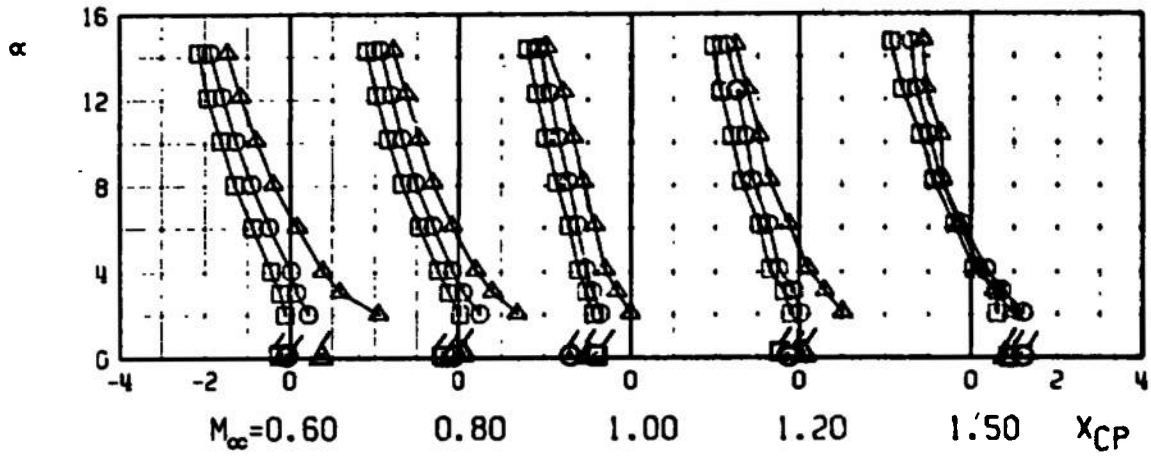

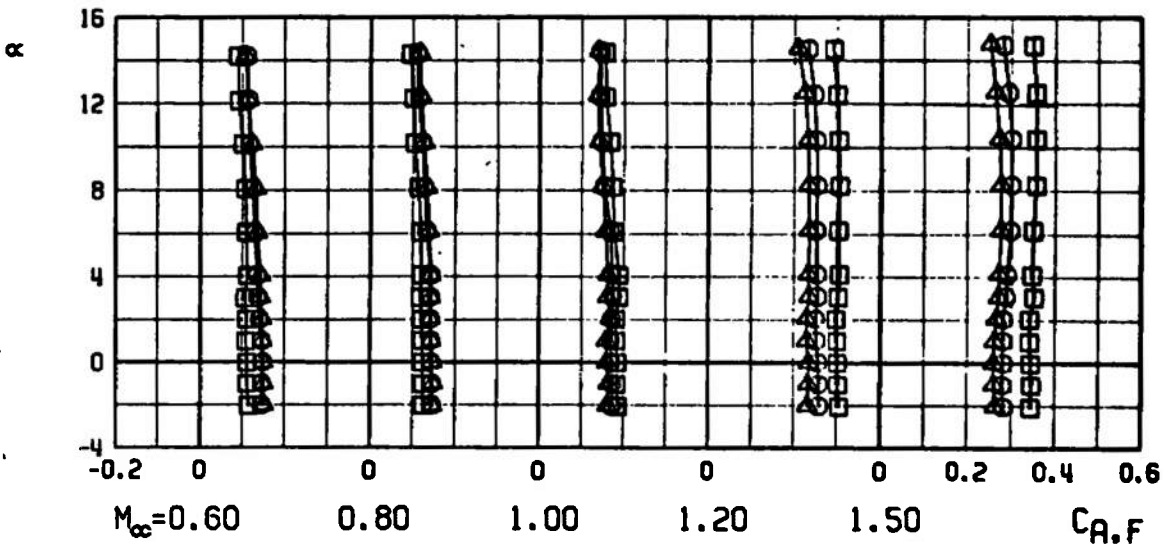

c. 0.50 Bluntness Ratio
Fig. 12 Continued

SYMBOL	CONF	BLUNTNESS
◻	N17 M9 A17	0.75
⊙	N21 M9 A17	0.75
△	N25 M9 A17	0.75

FLAGGED SYMBOLS REPRESENT NEUTRAL POINT LOCATION

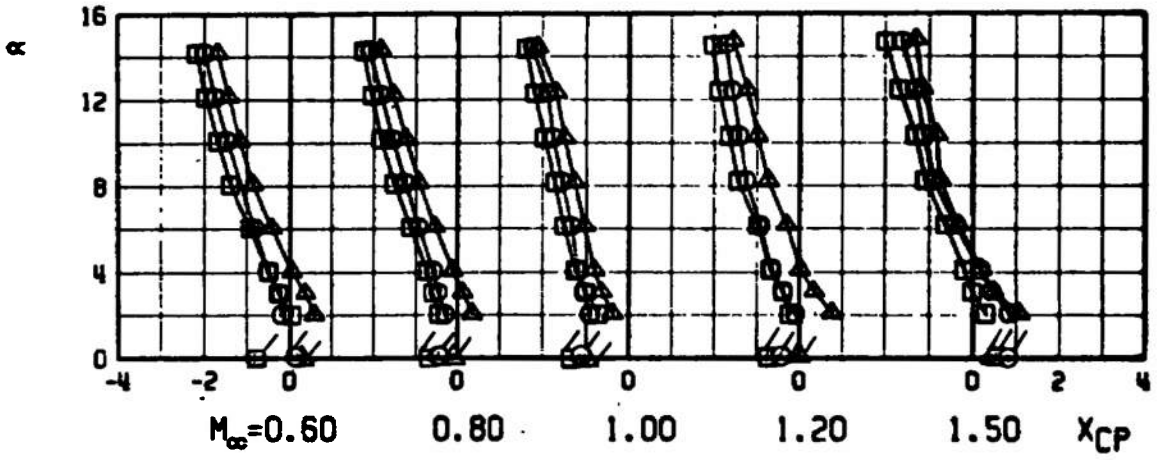

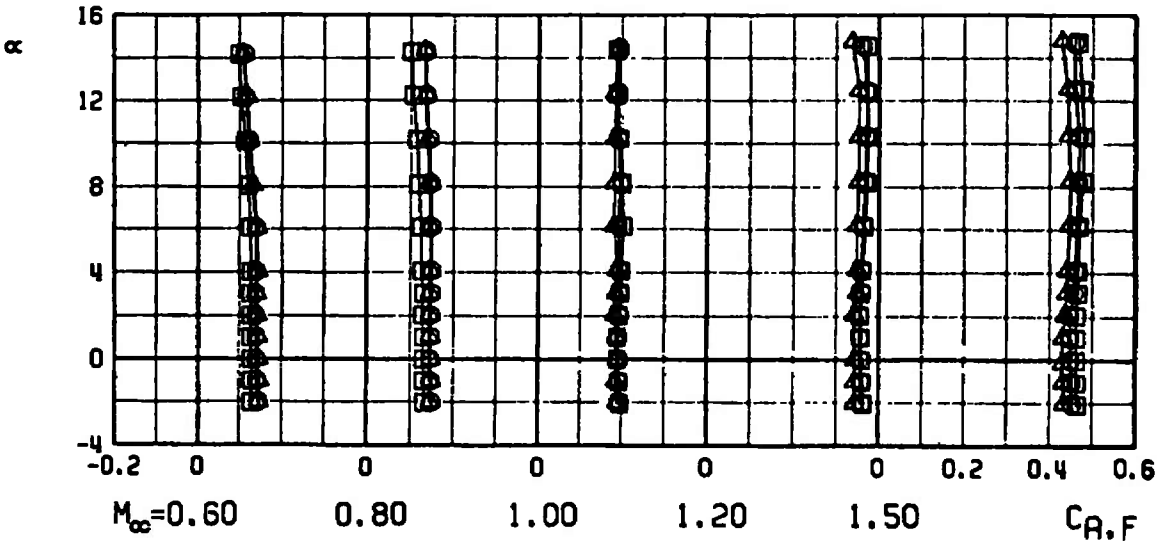

d. 0.75 Bluntness Ratio
Fig. 12 Concluded

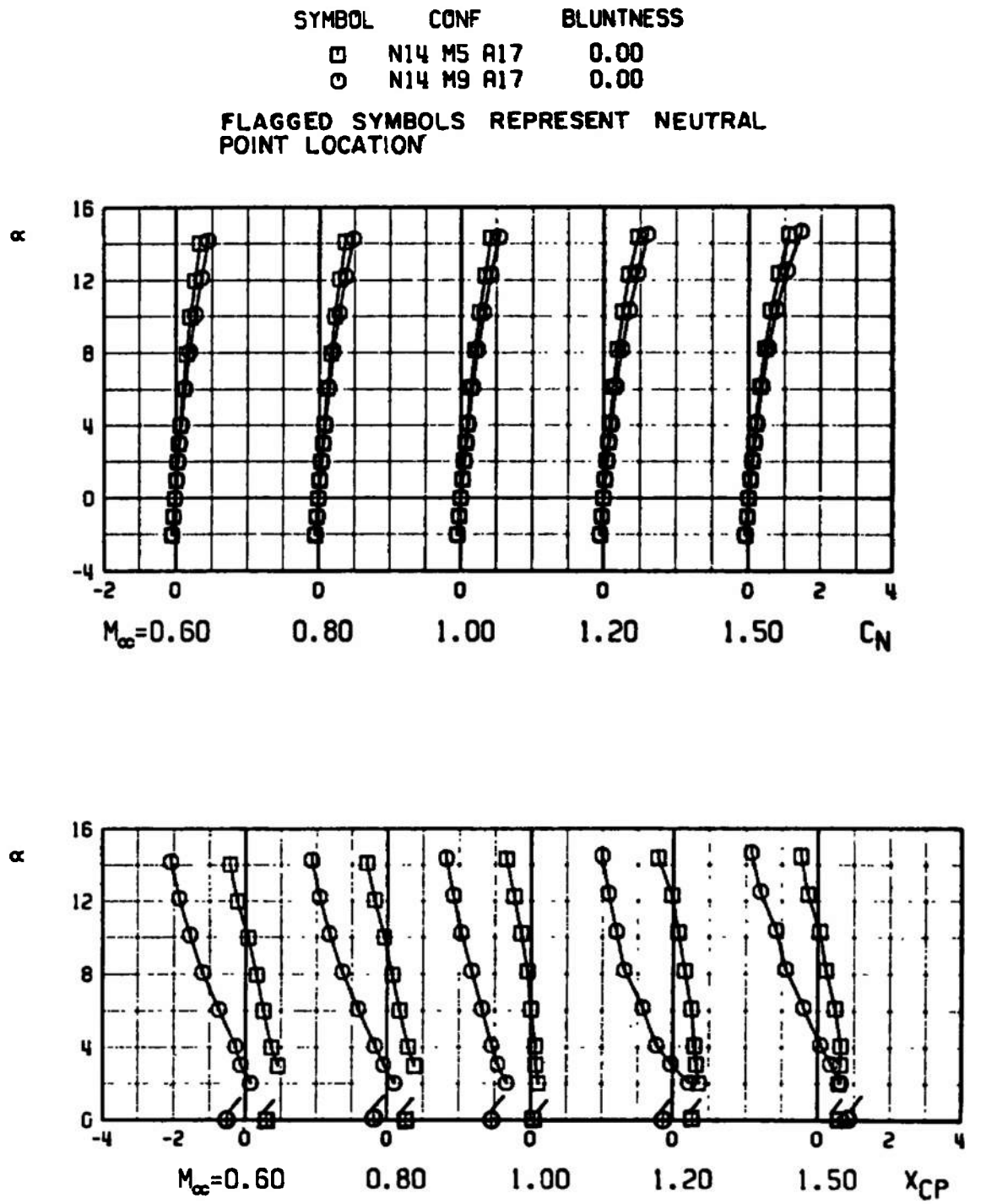

a. Normal-Force Coefficient and Center-of-Pressure Location, Zero Bluntness Ratio

Fig. 13 Aerodynamic Coefficients of 5- and 9-cal Midbodies Fitted with 2-cal Noses

SYMBOL	CONF	BLUNTNESS
□	N14 M5 A17	0.00
○	N14 M9 A17	0.00

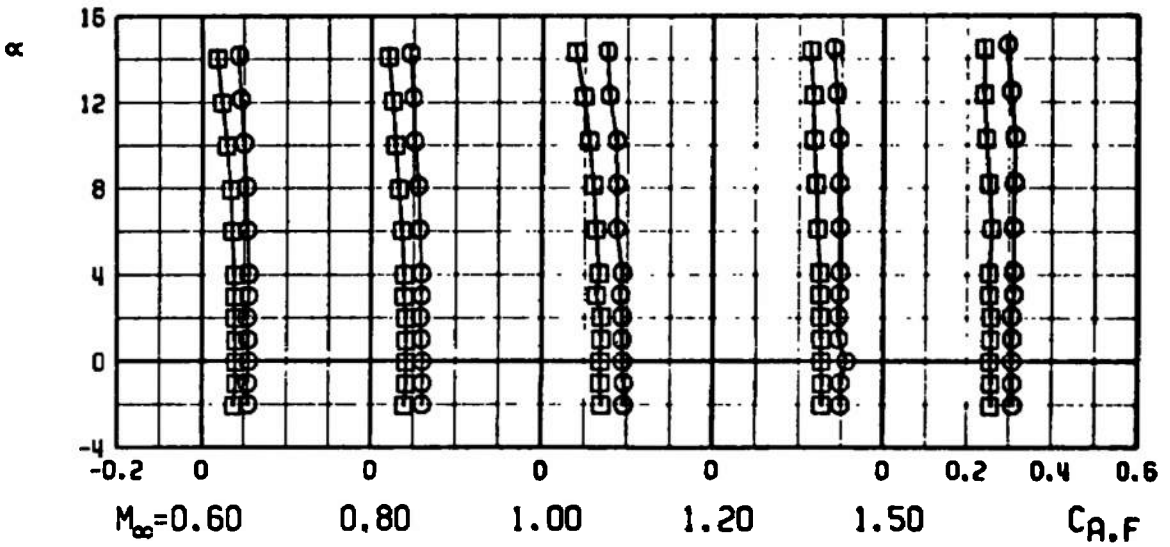

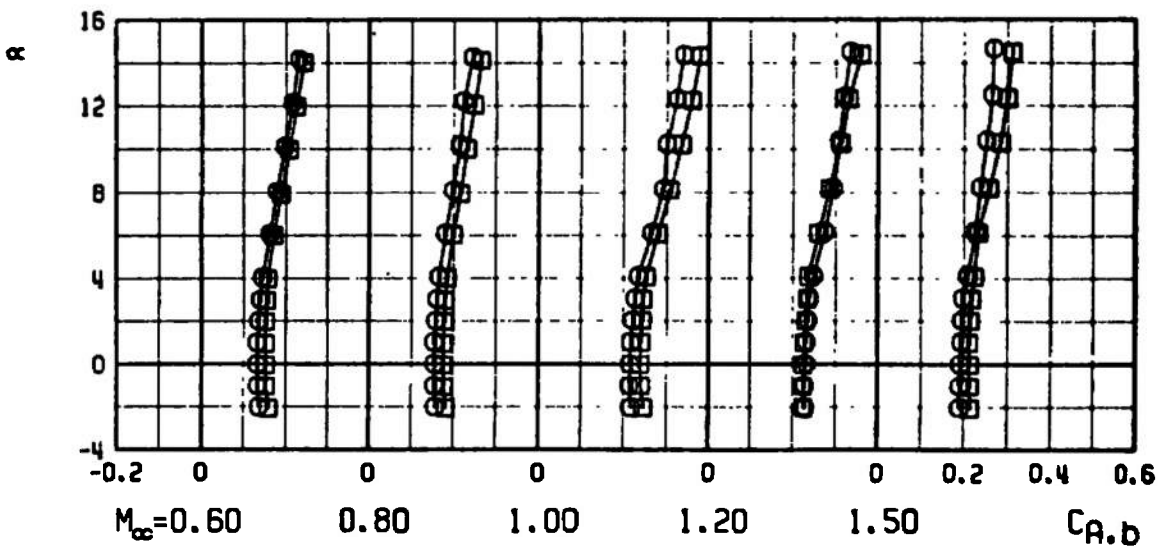

b. Forebody and Base Axial-Force Coefficients, Zero Bluntness Ratio
Fig. 13 Continued

SYMBOL	CONF	BLUNTNESS
□	N16 M5 A17	0.50
○	N16 M9 A17	0.50

FLAGGED SYMBOLS REPRESENT NEUTRAL POINT LOCATION

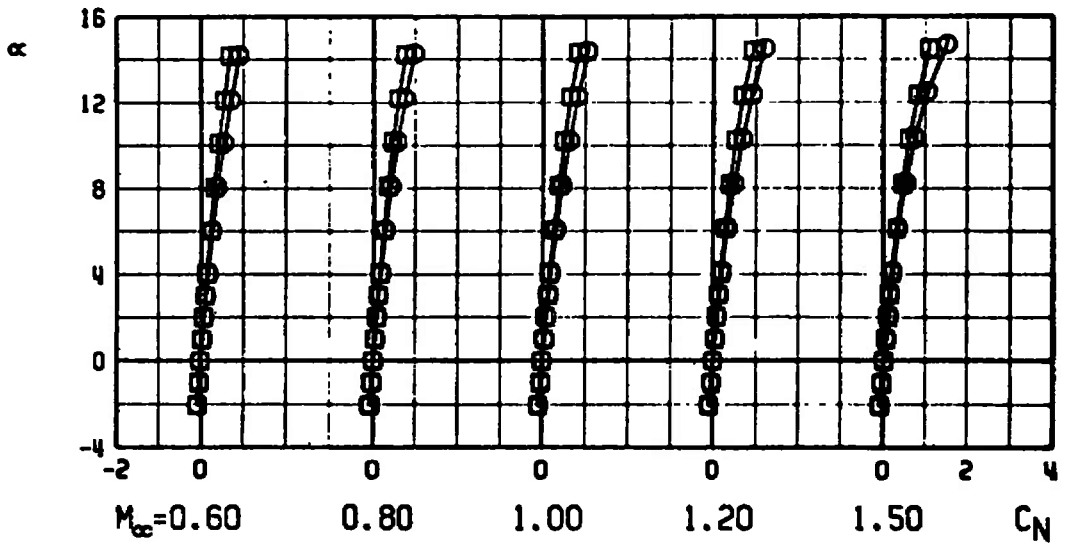

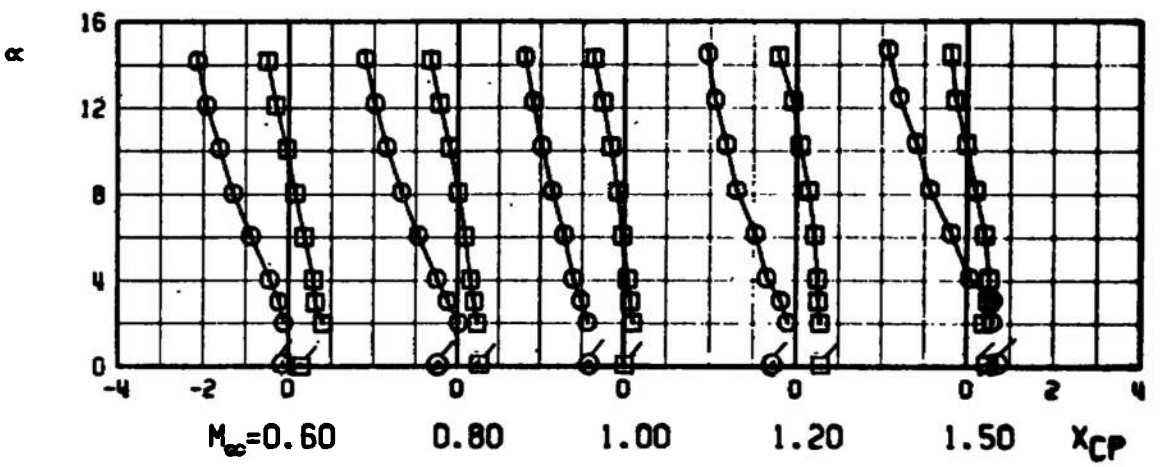

c. Normal-Force Coefficient and Center-of-Pressure Location, 0.50 Bluntness Ratio
Fig. 13 Continued

SYMBOL	CONF	BLUNTNESS
□	N16 M5 A17	0.50
○	N16 M9 A17	0.50

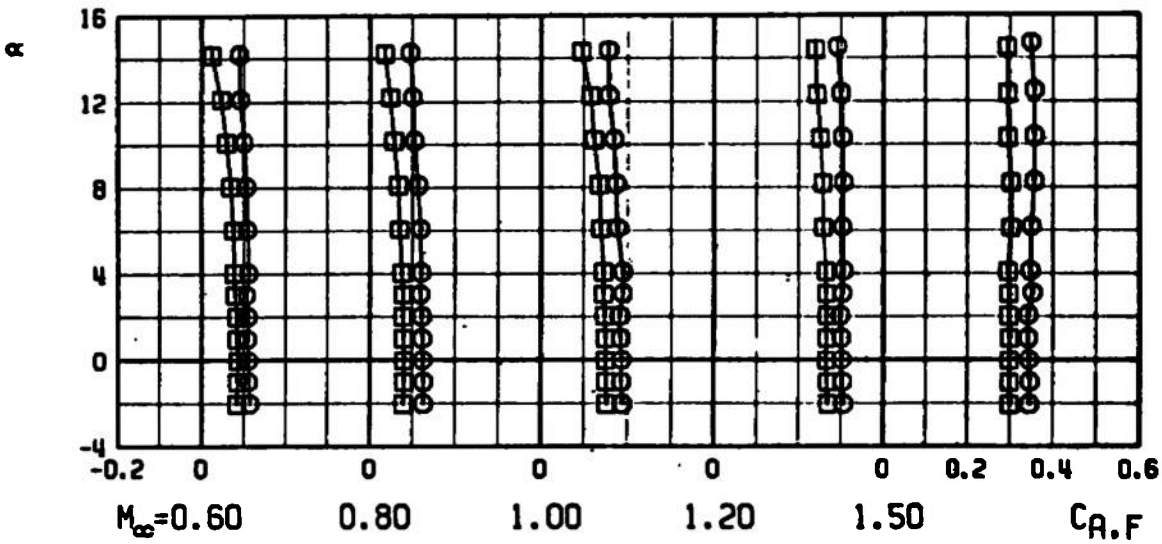

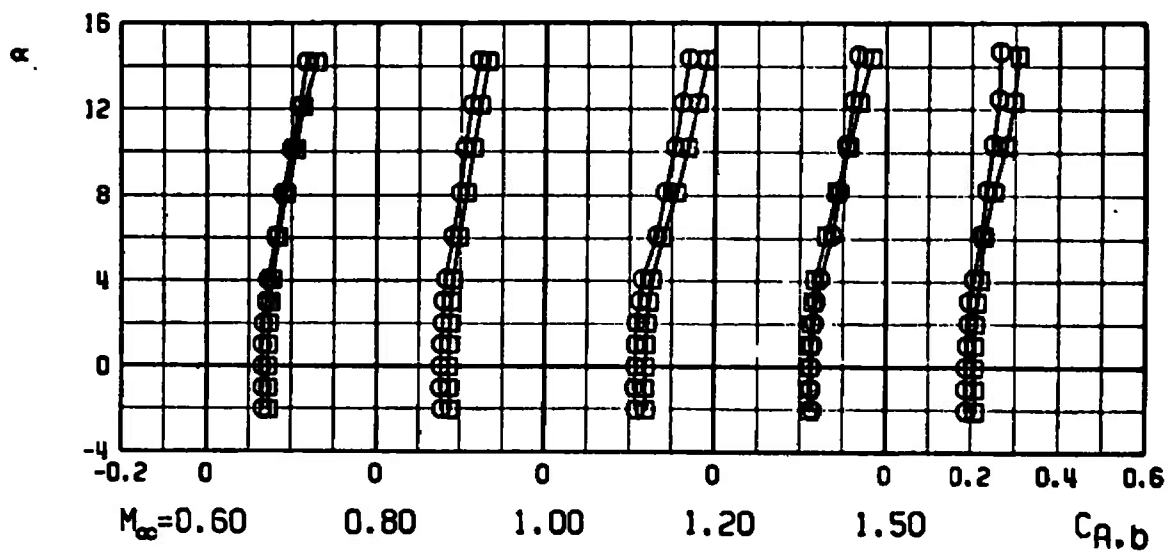

d. Forebody and Base Axial-Force Coefficient, 0.50 Bluntness Ratio
Fig. 13 Concluded

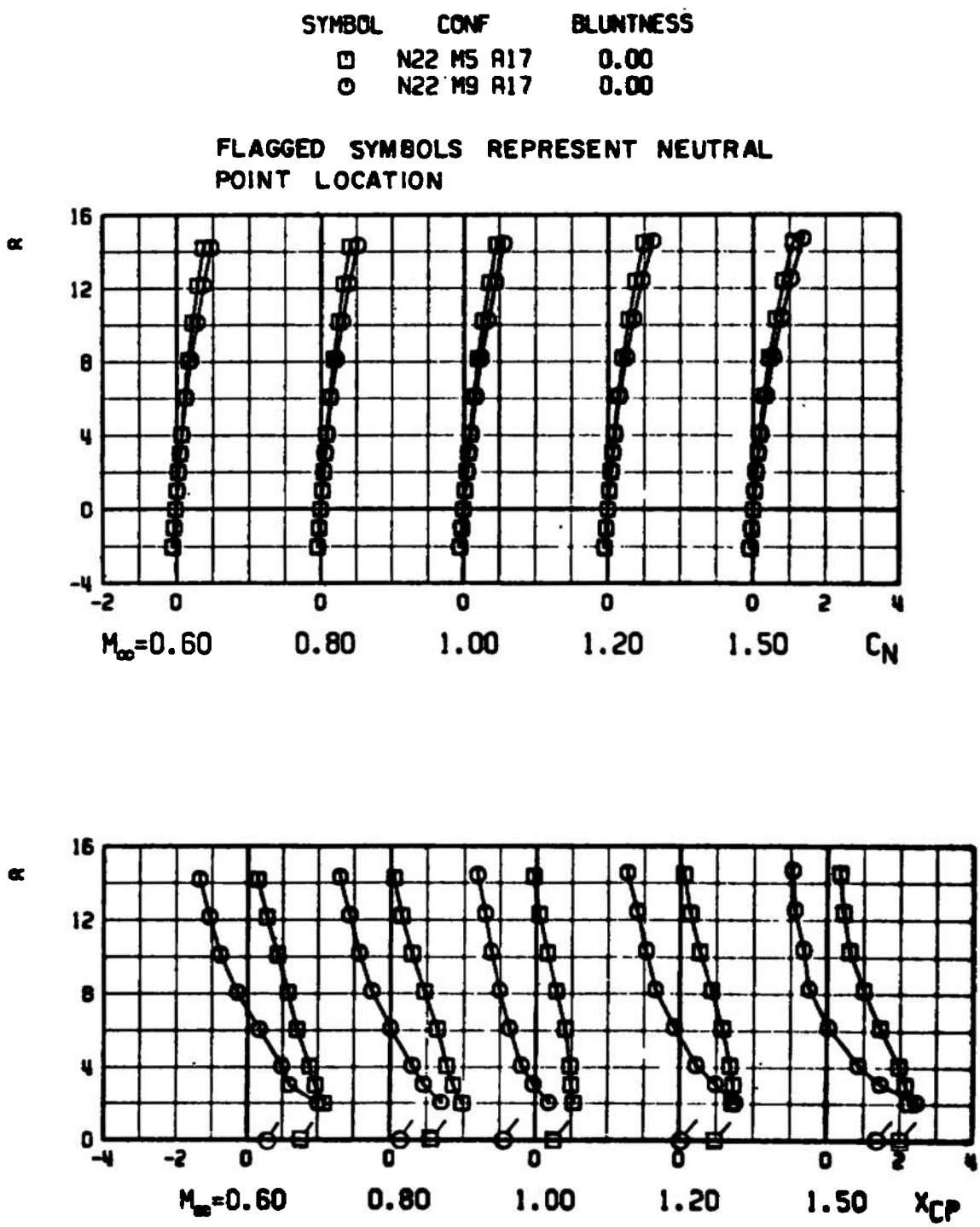

a. Normal-Force Coefficient and Center-of-Pressure Location, Zero Bluntness Ratio

Fig. 14 Aerodynamic Coefficients of 5- and 9-cal Midbodies Fitted with 4-cal Noses

SYMBOL	CONF	BLUNTNESS
⊡	N22 M5 A17	0.00
⊙	N22 M9 A17	0.00

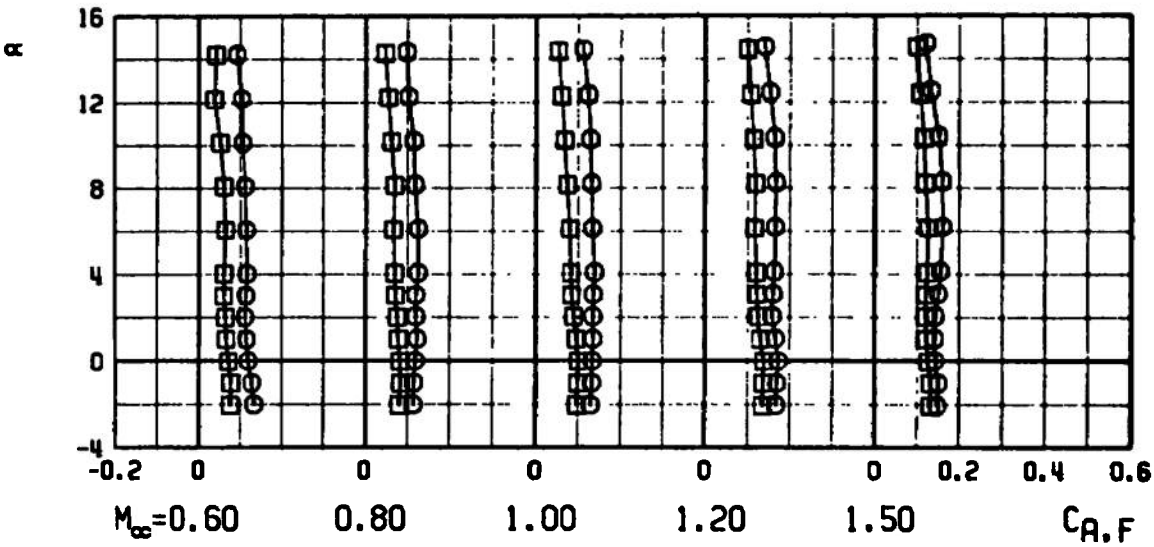

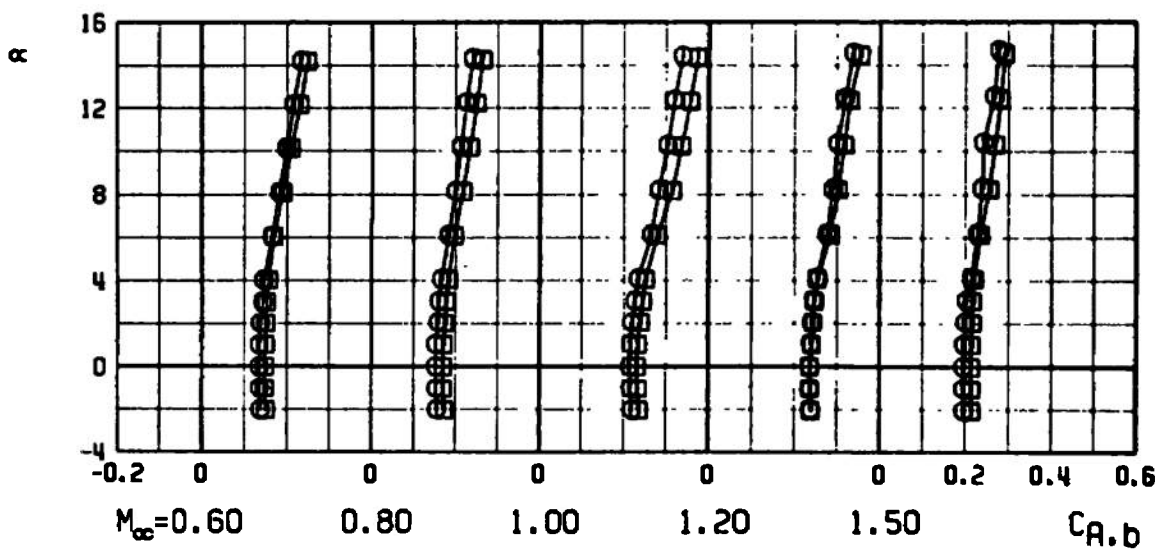

b. Forebody and Base Axial-Force Coefficients, Zero Bluntness Ratio
Fig. 14 Continued

SYMBOL	CONF	BLUNTNESS
⊡	N24 M5 A17	0.50
⊙	N24 M9 A17	0.50

FLAGGED SYMBOLS REPRESENT NEUTRAL POINT LOCATION

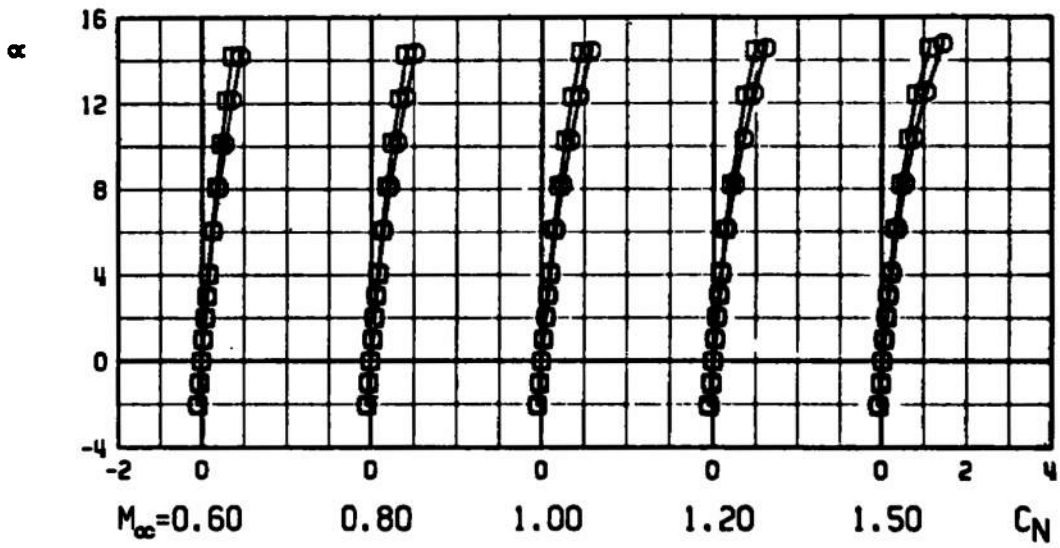

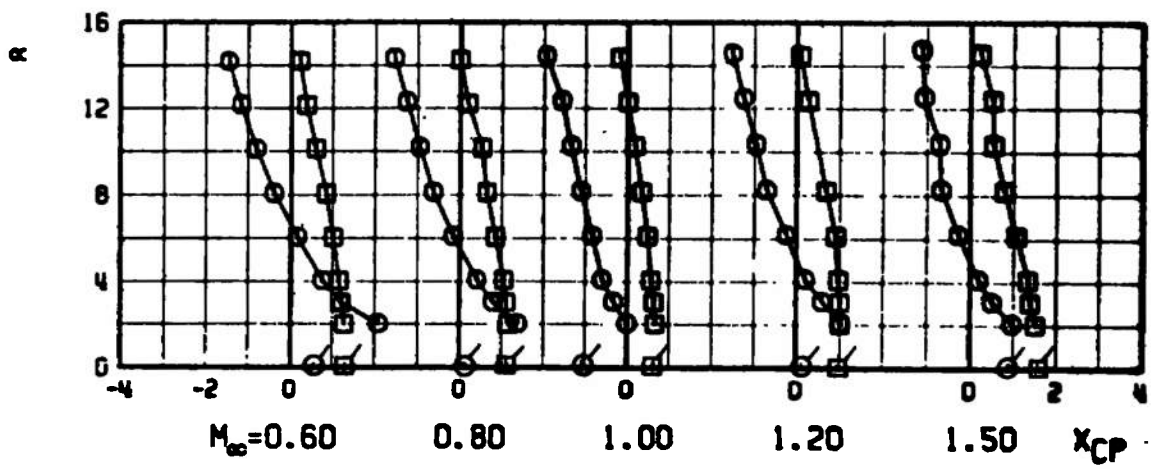

c. Normal-Force Coefficient and Center-of-Pressure Location, 0.50 Bluntness Ratio
Fig. 14 Continued

SYMBOL	CONF	BLUNTNESS
□	N24 M5 A17	0.50
○	N24 M9 A17	0.50

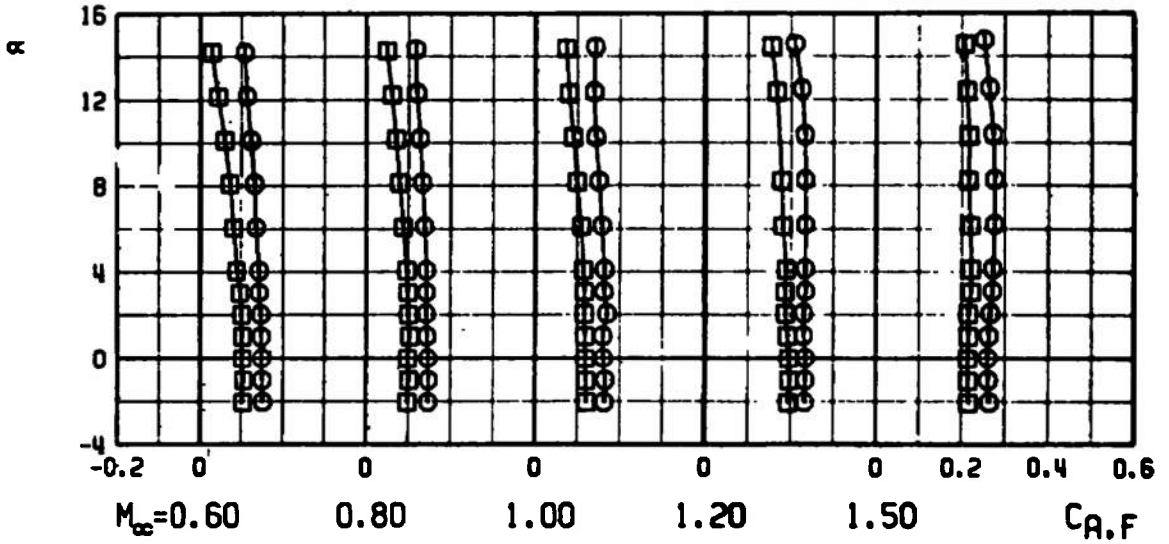

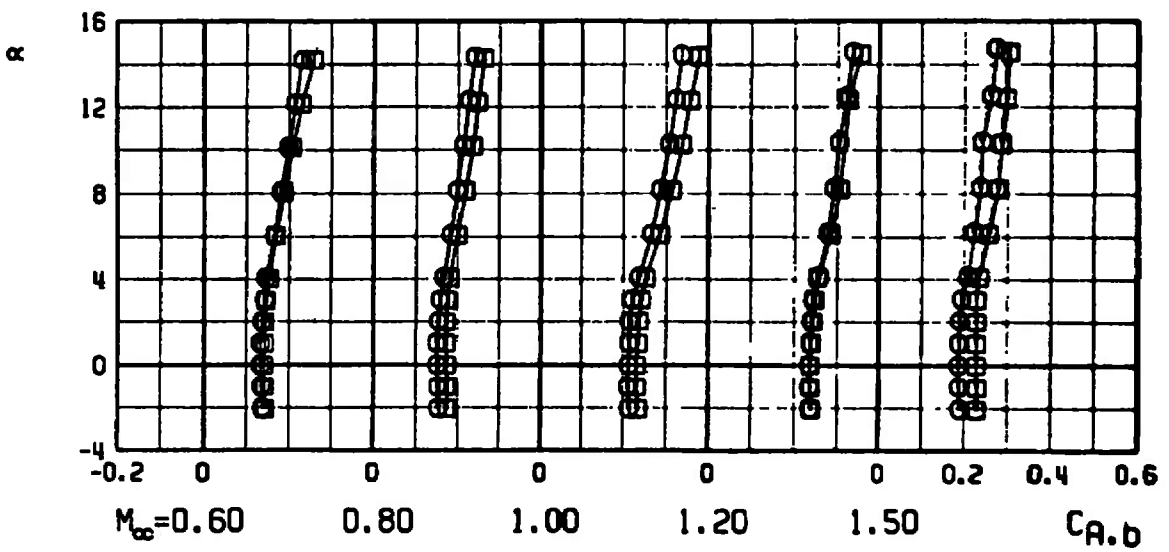

d. Forebody and Base Axial-Force Coefficients, 0.50 Bluntness Ratio
Fig. 14 Concluded

UNCLASSIFIED

Security Classification

DOCUMENT CONTROL DATA - R & D

(Security classification of title, body of abstract and indexing annotation must be entered when the overall report is classified)

1 ORIGINATING ACTIVITY *(Corporate author)*

Arnold Engineering Development Center
Arnold Air Force Station, Tennessee

2a. REPORT SECURITY CLASSIFICATION: UNCLASSIFIED

2b GROUP: N/A

3 REPORT TITLE

AERODYNAMIC CHARACTERISTICS OF TWO BODIES OF REVOLUTION WITH NOSES OF VARYING SPHERICAL BLUNTNESS AT MACH NUMBERS FROM 0.6 TO 1.5

4 DESCRIPTIVE NOTES *(Type of report and inclusive dates)*

November 29 through December 13, 1972--Final Report

5 AUTHOR(S) *(First name, middle initial, last name)*

E. G. Allee, Jr., ARO, Inc.

6 REPORT DATE	7a. TOTAL NO OF PAGES	7b. NO. OF REFS
April 1973	51	1

8a. CONTRACT OR GRANT NO

b. PROJECT NO 2547

c. Program Element 62602F

d.

9a. ORIGINATOR'S REPORT NUMBER(S)

AEDC-TR-73-44

AFATL-TR-73-50

9b. OTHER REPORT NO(S) *(Any other numbers that may be assigned this report)*

ARO-PWT-TR-73-9

10 DISTRIBUTION STATEMENT

Approved for public release; distribution unlimited.

11 SUPPLEMENTARY NOTES

Available in DDC

12 SPONSORING MILITARY ACTIVITY

AFATL/DLGC
Eglin Air Force Base
Florida 32542

13 ABSTRACT

A wind tunnel investigation was conducted in the Aerodynamic Wind Tunnel (1T) to determine the static stability characteristics of two bodies of revolution fitted with 2-, 3-, and 4-cal tangent ogive noses of varying spherical bluntness. Testing was conducted at Mach numbers from 0.6 to 1.5 and angles of attack from -2 to 14 deg. The major effect of blunting the noses was evidenced in the axial-force coefficient. Lengthening the noses from 2 to 4 cal caused a forward movement of the center-of-pressure location and a corresponding decrease in axial-force coefficient at Mach numbers of 1.0 and higher. Changing from a 5- to a 9-cal midbody resulted in an increase in axial-force coefficient and an aft movement of the center-of-pressure location.

DD FORM 1 NOV 68 1473

UNCLASSIFIED

Security Classification

14. KEY WORDS	LINK A		LINK B		LINK C	
	ROLE	WT	ROLE	WT	ROLE	WT
aerodynamic characteristics						
bodies of revolution						
blunt bodies						
center of pressure						
transonic flow						